ZIRCONIUM PHOSPHATE/IONIC LIQUID PROTON CONDUCTORS FOR HIGH TEMPERATURE FUEL CELL APPLICATIONS

by

Hanin Mohammed

A Thesis presented to the Faculty of the
American University of Sharjah
College of Engineering
In Partial Fulfillment
of the Requirements
for the Degree of

Master of Science in
Chemical Engineering

Sharjah, United Arab Emirates

November 2017

Approval Signatures

We, the undersigned, approve the Master's Thesis of Hanin Mohammed

Thesis Title: Zirconium Phosphate/Ionic Liquid Proton Conductors for High Temperature Fuel Cell Applications.

Signature	**Date of Signature** (dd/mm/yyyy)
Dr. Amani Al-Othman Assistant Professor, Department of Chemical Engineering Thesis Advisor	
Dr. Paul Nancarrow Associate Professor, Department of Chemical Engineering Thesis Co-Advisor	
Dr. Rana Sabouni Assistant Professor, Department of Chemical Engineering Thesis Committee Member	
Dr. Yehya El-Sayed Associate Professor, Department of Biology, Chemistry and Environment Thesis Committee Member	
Dr. Naif Darwish Head, Department of Chemical Engineering	
Dr. Ghaleb Husseini Associate Dean for Graduate Affairs and Research College of Engineering	
Dr. Richard Schoephoerster Dean, College of Engineering	
Dr. Mohamed El-Tarhuni Vice Provost for Graduate Studies	

Acknowledgments

First and foremost, all praises to almighty Allah for giving me the strength and ability to complete this work and for all his blessings in every step of my life.

Second, I would like to express my deepest gratitude to my advisors Dr. Amani Al-Othman and Dr. Paul Nancarrow for their endless and continuous support throughout each stage of the research work. I thank them for their valuable comments and encouragements during the past two years.

Moreover, I would like to deeply thank Dr. Yehya El Sayed for his help, support and valuable discussions and suggestions. I also thank Mr. Ziad Sara for his help in performing the FTIR analysis. I sincerely thank Eng. Muhammad Qasim for his lab help and valuable suggestions.

I would also like to thank University of Sharjah for their help in performing the XRD, Raman spectroscopy, high temperature test and SEM.

I deeply thank the American University of Sharjah (AUS) and Dr. Naif Darwish for providing me with Graduate Teaching Assistantship during my graduate studies.

Finally, I would like to warmly thank my beloved parents and my brothers for their endless love and support and non-stop encouragements throughout this research.

Dedication

To my beloved mother …

Abstract

High temperature operation (> 120 °C) is preferred in proton exchange membrane (PEM) fuel cells. It enhances the electrode kinetics, improves the catalyst tolerance for impurities and allows the use of lower cost fuels such as hydrocarbons. However, high temperature operation is not possible using the conventional Nafion membranes. Their proton conductivity decreases dramatically beyond 90 °C. Therefore, this work aimed at developing Nafion-free proton conducting material, based on zirconium phosphates (ZrP) and ionic liquids (IL) to allow a high temperate operation. ZrP/IL proton conducting–materials were prepared via the reaction of zirconium oxychloride $ZrOCl_2$ in an aqueous solution with phosphoric acid H_3PO_4 at room temperature. Seven different ionic liquids, were investigated in this work. The ionic liquid component was added to the $ZrOCl_2$ solution prior to the precipitation reaction with IL contents ranging from 0.4-5% by mass. The modified materials were investigated for their proton conductivity. The results of this work demonstrated that the addition of ionic liquids enhances the proton conductivity of the ZrP material by orders of magnitude. Among all the tested ionic liquids, 1-ethyl-3-methylimidazolium ethyl sulfate, 1-butyl-3-methylimidazolium dicyanamide, and 1-butyl-3-methylimidazolium triflate produced the best results with conductivities of 2.26×10^{-2}, 1.61×10^{-2} and 1.36×10^{-2} S cm^{-1}, respectively. The proton conductivity of the unmodified ZrP prepared in this work was equal to 9.24×10^{-4} S cm^{-1}. The modified samples were analyzed by thermogravimetric analysis (TGA), X-ray diffraction (XRD), Fourier transform infrared spectroscopy (FTIR), Raman spectroscopy and scanning electron microscopy (SEM). Results showed the enhancement of water uptake properties by 40-60%, changes in morphology and changes in structure upon the introduction of the IL component. The modified samples were processed at high temperature (200 ºC) under completely anhydrous conditions and showed a high anhydrous proton conductivity on the order of 10^{-4} S cm^{-1}. In conclusion, it appeared that the ionic liquids have formed hydrogen bonds with the ZrP molecules and hence, provided additional pathways for the proton transfer and effective proton hopping sites. The enhanced conductivity of the ZrP/IL materials make them good candidates as solid proton conductors for fuel cells applications.

Search Terms: Polymer electrolyte membrane fuel cells, proton conductivity, zirconium phosphate and ionic liquids.

Table of Contents

List of Tables

List of Figures

Nomenclature

AFC	Alkaline fuel cells
[BMIM][DCA]	1-butyl-3-methylimidazolium dicyanamide
[BMIM] [OTF]	1-butyl-3-Methylimidazolium triflate
[BMIM] [TFA]	1-ethyl-3-methylimidazolium trifluoroacetate
DHFC	Direct hydrocarbon fuel cells
[DEMA][OMS]	diethylmethylammonium methanesulfonate
[DEMA][OTF]	diethylmethylammonium trifluoromethanesulfonate
EIS	Electrochemical impedance spectroscopy
[EMIM][AC]	1-ethyl-3-methylimidazolium acetate
[EMIM][ESO_4]	1-ethyl-3-methylimidazolium ethyl sulfate
FC	Fuel cells
FTIR	Fourier transform infrared spectroscopy
GLY	Glycerol
IL	Ionic liquid
MCFC	Molten carbonate fuel cells
PAFC	Phosphoric acid fuel cells
PEM	Polymer electrolyte membrane or proton exchange membrane
PEMFC	Polymer electrolyte membrane fuel cells
SEM	Scanning electron microscopy
SOFC	Solid oxide fuel cells
TGA	Thermogravimetric analysis
XRD	X-ray diffraction
ZrP	Zirconium hydrogen phosphate (zirconium phosphate

Chapter 1. Introduction

1.1. Overview

Global warming and air pollution are two main challenges that threaten human health and political stability [1]. Due to the excessive use of fossil fuels for energy and material production in the last two decades, the earth is experiencing an increase in global temperatures and climate change. As a result of their combustion, fossil fuels emit greenhouse gases, mainly CO_2, which contributes to the global warming issue [2]. Accordingly, the need for a cleaner yet, efficient energy sources is required. Fuel cells are one of the most promising sources of a clean energy considering their low nitrogen and sulfur oxide emissions and their low noise levels [3].

A fuel cell is a device that converts chemical energy directly into electrical energy using a continuously supplied fuel and oxidant [4]. The idea of fuel cells was first described by Sir William Grove in 1893 [5]. He described a hydrogen/oxygen fuel cell that consisted of a platinized platinum electrode immersed in sulfuric acid [6]. One of the limitations of Grove's cell was the limited current it produced as a result of the small effective area of the Pt electrode in the cell [7]. In 1889, Ludwig Mond and his assistant Carl Langer started an experiment to increase the "surface of action" of the cell. They used a porous matrix to contain the liquid electrolytes. They also initiated the use of powdered electrocatalysts such as platinum black [8]. In 1893, Friedrich Wilhelm Ostwald determined the relation between the different components in a fuel cell: the electrodes, the electrolytes, the anions and cations [9]. Francis Bacon, in 1932, modified the Mond and Langer model, which led later to the development of the first alkali fuel cell [10]. By the end of the 1950s, Francis Bacon developed a 6 kW fuel cell stack [11]. The first practical fuel cell, however, was used in the U.S. space program. General Electric (GE) developed the first polymer electrolyte membrane (PEM) fuel cells in the early 1960s, which was used in the Gemini program [12]. Thomas Grubb and Leonard Niedrach used sulfonated polystyrene membranes, but these were replaced by Nafion in 1966 [13]. In 1986, D.S Watkins, one of the developers at the Ballard organization, found that an experimental membrane made up by DOW chemicals had the ability to increase the PEM fuel cell power by four times [14]. Figure 1 shows a timeline that gives a summary of the fuel cell development.

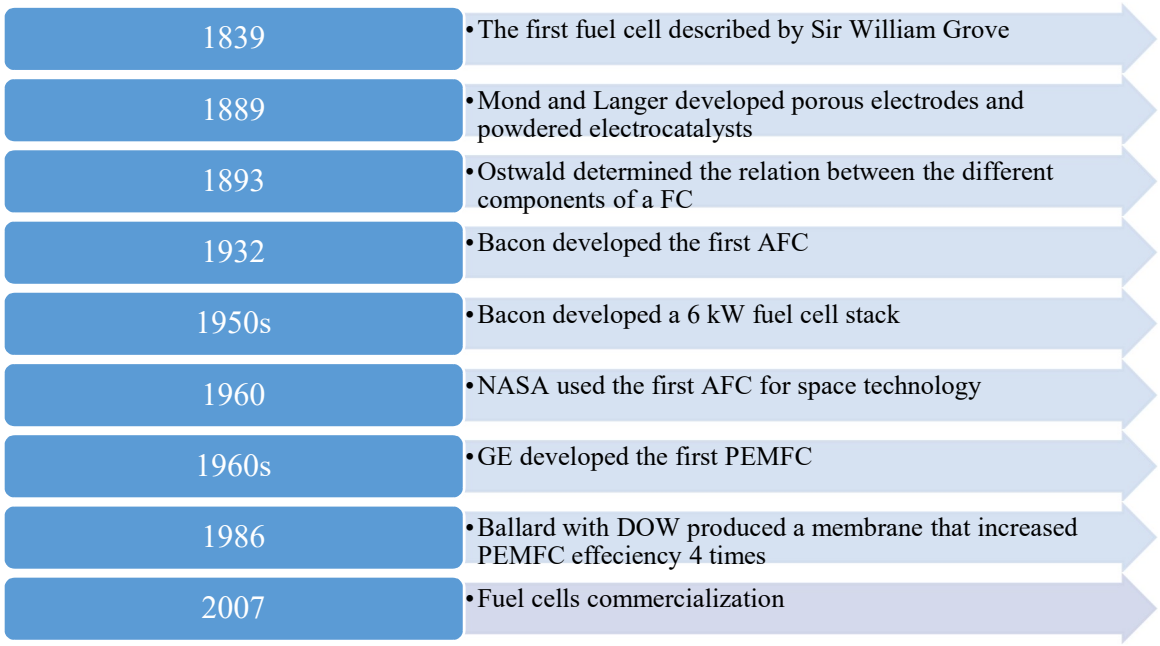

Figure 1. Timeline for fuel cell development

Fuel cells can be classified based on their electrolyte material into five types: phosphoric acid, alkaline, solid oxide, molten carbonate, and proton exchange membrane or polymer electrolyte membrane PEM fuel cells (PEMFC). Among these, PEMFCs offer excellent performance using hydrogen or methanol as fuels. They possess an all-solid structure (referring to the solid electrolyte) that makes them perfect candidates for many applications.

Nafion, manufactured by Dupont, is the most widely used membrane in PEMFCs [15]. This perfluorosulfonic acid membrane functions well, at temperatures around 80 ºC and fully hydrated conditions, displaying a proton conductivity of 0.1 S cm^{-1} [16]. However, as the temperature increases, Nafion dehydrates and its proton conductivity dramatically decreases [15]. High temperature operation is preferred in PEMFCs for several reasons. It enhances the electrochemical reaction kinetics for the fuel cell, improves water management and, increases the fuel cell tolerance for impurities such as carbon monoxide (CO), hence, allows the use of a more variety of fuels and catalysts [17, 18]. Unfortunately, increasing the operating temperature is not permitted with the use of Nafion membranes.

Hydrogen is the most commonly used fuel in PEM fuel cells as it has the highest current density of all types of fuels [14]. Hydrocarbons offer many attractive features as opposed to hydrogen. They have higher energy storage density, and are easier to

store and transport. Hydrocarbon fuels have a well-established infrastructure. For example, Propane is distributed by trucks in North America to rural locations while natural gas is distributed by pipelines into urban areas. The use of hydrocarbons as fuel eliminates the fuel processor unit and decreases the cost of PEMFCs. The advantages of hydrocarbons appear to be substantial; however, their reaction rates are extremely small at low temperatures [19]. As a result, high temperature operation is required. With their lower cost and existing infrastructure, it appears that there is a merit to use hydrocarbon fuels in PEMFCs. In order to use such fuels, the operating temperature of PEMFCs should be increased. Current perflourosulfonic acid membranes cannot be operated at temperatures beyond 90^{o}C. Hence, there is an immense effort to develop high temperature proton conducting membranes. These efforts have achieved moderate success so far.

Ionic liquids incorporated in Zirconium hydrogen phosphate $Zr(HPO_4)_2$ (ZrP) are investigated in this project as a solid protonic conductor that can replace the current perfluorosulfonic acid membranes. Zirconium hydrogen phosphate $Zr(HPO_4)_2$ (ZrP) has been studied since the 60's of the last century and characterized by its layered structure and ion-exchange properties. It has good proton conductivity at temperatures higher than 120 °C [20]. ZrP composite membranes have also showed reasonable proton conductivities at high temperatures [21]. Novel membranes based on ZrP polytetrafluoroethylene (PTFE) and, Glycerol (GLY), were reported in the literature [22]. ZrP was also successfully incorporated in perfluorosulfonic acid membranes, e.g. Nafion [23].

Ionic liquids are salts, typically consisting of organic cations and inorganic anions, that exist in the liquid phase at ambient temperatures. They have attracted increasing attention over the past decade for a wide range of applications due to their unique physical and chemical properties. In particular, ionic liquids are of significant interest in electrochemical energy applications, due to their wide electrochemical and thermal stabilities, negligible volatilities and high ionic conductivities [24].

1.2. Thesis Objectives

This work is aimed at developing a Nafion-free proton conducting material, based on zirconium phosphates (ZrP), ionic liquids and glycerol as a possible electrolyte material for direct hydrocarbon PEMFCs. Direct hydrocarbon fuel cells are proposed to satisfy electricity needs in modest quantities for the residents of rural areas and certain portable applications.

The main objectives of this study are to:

1- Synthesize novel proton conducting materials based on ionic liquids (ILs) and zirconium phosphate.
2- Investigate the proton conductivity of the synthesized zirconium phosphate/ionic liquid material.
3- Study and optimize the content of ionic liquids, that provides the highest proton conductivity, in modified zirconium phosphates.
4- Evaluate the properties of the synthesized material including their proton conductivity via electrochemical impedance spectroscopy (EIS), morphology, structure and water uptake characteristics using various analysis techniques including: Thermogravimetric analysis (TGA), Fourier-transform infrared spectroscopy (FTIR), Raman spectroscopy, scanning electron microscopy (SEM), and X-ray diffraction (XRD).

A sub-objective of this study is to synthesize novel proton conducting materials based on glycerol and zirconium phosphate and investigate its proton conductivity, thermal stability, water uptake and morphology.

1.3. Thesis Organization

This thesis is divided into six chapters. Chapter one is the thesis introduction. It includes an overview of the project, the problem statement and the objectives of the study. Chapter two includes an extensive literature review about applications of fuel cells, different types of fuel cells and direct hydrocarbon fuel cells (DHFC). It also provides information about the currently used proton conductors and the suggested alternative electrolyte materials for PEM fuel cells, including zirconium phosphate, glycerol, and ionic liquids. Chapter three deals with the materials and detailed experimental methodology used to carry out this project. Chapter four presents the

experimental results on the study and development of the proton conducting materials. It also provides a detailed analysis and discussion for the findings in this research. Chapter five presents the results and discussion for the incorporation of glycerol in the ZrP material. Chapter six includes the conclusions and recommendations for future work.

Chapter 2. Literature Review

2.1. Fundamentals of Fuel Cells

A fuel cell is composed of a conducting electrolyte, a cathode and an anode. This layer combination is called the membrane-electrode assembly (MEA) [25]. As an illustration, a schematic diagram of a PEMFC is shown in Figure 2. The fuel, such as hydrogen, is continuously fed to the anode where an electro-oxidation reaction occurs, and hydrogen ions and electrons are released. The electrons are forced to move toward the cathode through an external circuit. The hydrogen ions (protons) diffuse through the electrolyte membrane toward the cathode. Hence, the membrane does not only separate the anode from the cathode but also acts as a proton conductive medium. At the cathode, the oxidant, O_2 (or oxygen in air) is fed. Oxygen is reduced by the coming electrons from the anode, to form O^{2-} which combines with H^+ to form water. The final products of the PEM fuel cell reaction in this example are electricity, water and heat [26].

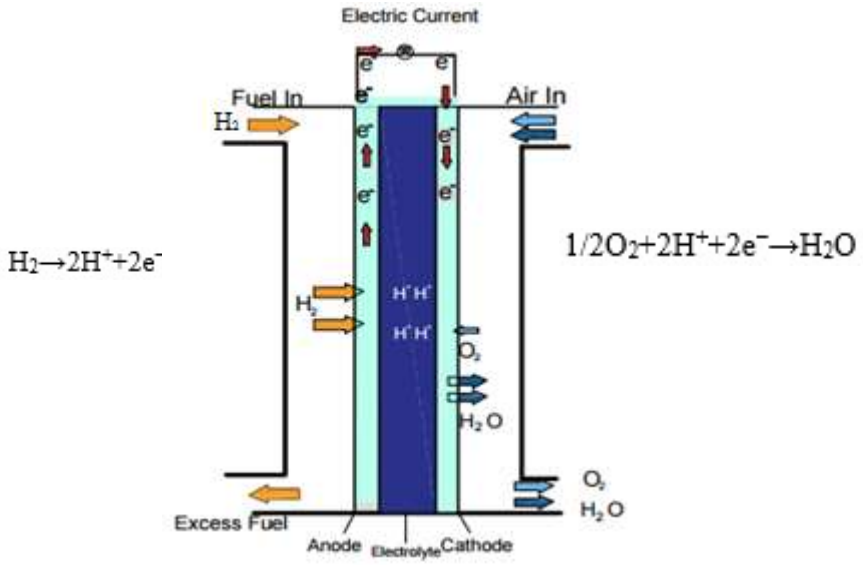

Figure 2. A schematic diagram of a fuel cell

If the fuel was a hydrocarbon, the electro-oxidation reactions in the fuel cell can be also illustrated as follows, taking propane (C_3H_8) as an example [27]:

$$C_3H_8 + 6\ H_2O \rightarrow 3\ CO_2 + 20\ H^+ + 20\ e^-$$

(1)

Oxygen or air enters the cathode, and the following reaction takes place:

$5\ O_2 + 20\ H^+ + 20\ e^- \rightarrow 10\ H_2O$

(2)

The overall reaction is:

$C_3H_8 + 5\ O_2 \rightarrow 3\ CO_2 + 4\ H_2O$

(3)

It can be seen that six moles of water are required for the reaction per one mole of propane reacted as per equation (1) for the anode side.

2.2. Types of Fuel Cells

Fuel cells are classified according to the type of the electrolyte material into five main types: alkaline fuel cells (AFC), molten carbonate fuel cells (MCFC), phosphoric acid fuel cells (PAFC), solid oxide fuel cells (SOFC) and proton exchange membranes fuel cells (PEMFC).

2.2.1. Alkaline fuel cells (AFCs)

The AFC is the oldest type of fuel cells [28]. AFCs use a liquid electrolyte solution of potassium hydroxide (KOH) and H_2 as a fuel. The reason behind choosing KOH is that it is the most conducting among all the alkaline hydroxides [29]. The main advantages of the AFC are: its high efficiency, as it gives the highest value among all other types, and its low cost [30]. Fast kinetics of the oxygen reduction are observed in the alkaline medium. This allows the use of inexpensive catalysts compared to the precious metal catalysts that are used in other types of fuel cells [31]. On the anode side, nickel can be used for the hydrogen oxidation reaction and silver can be used on the cathode [32]. One major disadvantage of the AFC is the intolerance to carbon dioxide (CO_2) [33]. When CO_2 is present in AFCs, it will react with the electrolyte material, KOH for example, producing carbonates [5]. This will result is a significant drop in the efficiency as the performance of AFCs depends on keeping the membrane in its pure form [5].

2.2.2. Molten carbonate fuel cells (MCFCs)

Molten carbonate fuel cells (MCFC) are high temperature fuel cells that operate in a temperature range of 550-700 ^oC. The high operating temperature permits the use of metallic cell components while keeping sufficient ionic conductivity in the cell [34]. Molten carbonate salt mixture suspended in a porous, chemically inert ceramic matrix

of beta-alumina is used as an electrolyte [35]. The anode and cathode in the MCFs are both made of nickel-based powders [36]. There are multiple fuel options for MCFCs which include: natural gases, bio-fuels and coal fuels [37]. The oxidant is usually O_2 mixed with CO_2 [38]. MCFCs possess a number of advantages: 1) they have a high efficiency and can be used as carbon capture and storage (CCS) systems [39], 2) they can be coupled to gas turbines to give an extremely efficient power generation due to their high operation temperature [40]. The high temperature eliminates the use of noble metal catalysts and therefore the overall operating costs are reduced [41]. However, there are some disadvantages associated with MCFCs such as hardware corrosion, low power density and cathode dissolution [42]. A typical MCFC is shown in Figure 3.

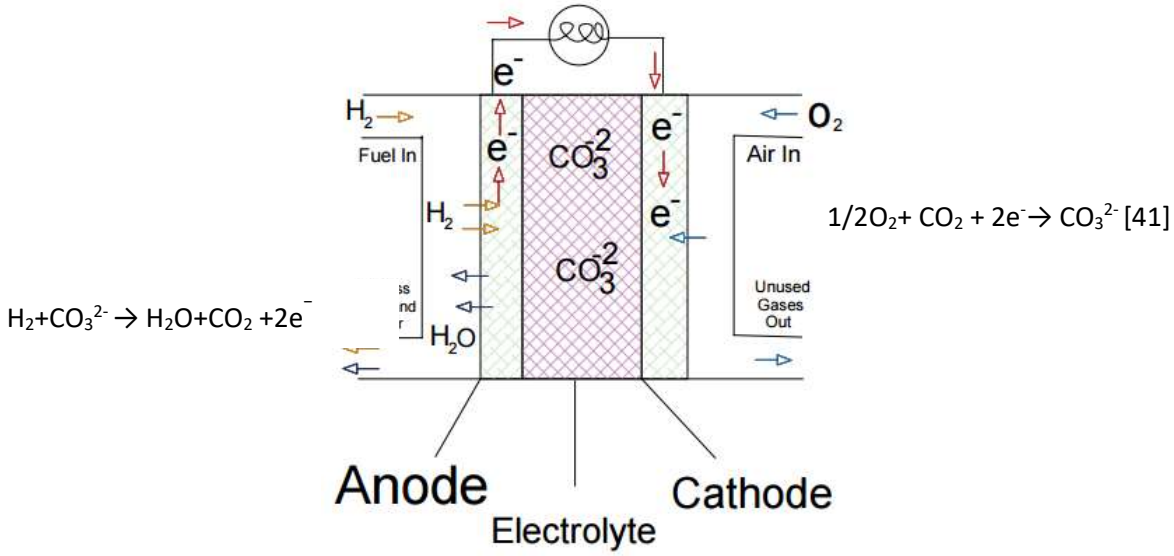

Figure 3. Molten carbonate fuel cell

2.2.3. Phosphoric acid fuel cells (PAFCs)

Phosphoric acid fuel cells (PAFC) are considered to be the most advanced and the most commercially used in many countries [43]. The operating temperature of PAFCs is around 200^{o}C [44]. This temperature is lower than the operating temperature in molten carbonate fuel cells and solid oxide fuel cells, but higher than that in proton exchange membranes fuel cells [45]. The electrolyte in PAFCs is H_3PO_4. The anode is composed of PTFE-bonded Pt/C, and the cathode, at which the oxidant is fed, is composed of 0.5 mg Pt/cm^2 in a graphite structure [46]. There are a number of advantages for PAFCs including: high stability, moderate temperature operation, low vapor pressure, ability to use air as an oxidant and high tolerance for carbon dioxide [47]. However, there are also some disadvantages associated with PAFCs mainly the

low power density compared to conventional combustion engines [48]. Moreover, PAFCs catalysts are noble metals which are expensive, they are intolerant to CO which causes anode poisoning and their electrolyte conductivity is considered low [49].

2.2.4. Solid oxide fuel cells (SOFCs)

Solid oxide fuel cells (SOFCs) are high temperature fuel cells that operate at a temperature range of 700ºC-1000ºC under atmospheric or pressurized conditions [50]. The most widely used electrolyte for SOFCs is yttria stabilized zirconia (YSZ) [51]. The cathode material must have certain characteristics in order to be suitable for SOFCs operation. These characteristics include: stability in the oxidizing environment, sufficient catalytic activity for oxygen reduction under operating conditions and good electronic conductivity [52]. (La,Sr)MnO_3 (LSM) is used as a cathode [53]. For the anode compartment, Ni-YSZ is used as it has a dual role of being a catalyst for hydrogen oxidation and being an electrical current conductor [54]. SOFCs demonstrate a lot of advantages that makes them suitable for a wide range of applications. SOFCs are considered the most efficient type of fuel cells, they produce high quality heat byproducts that can be used for co-generations or in combined cycle applications, they do not contain noble metals and they have a long life expectancy which ranges from 40000–80000 hours [55]. Moreover, the high operating temperature allows SOFCs to be flexible in terms of fuel selection. They operate with different types of fuels, regardless of their source whether from fuels or renewable energy, such as methanol, gasoline diesel, biogas, ethanol and syngas [56]. These advantages allowed SOFCs to be used in a variety of applications such as portable devices, small power systems, automotive auxiliary power, distributed generation power plants and residential power [57]. The main disadvantages of SOFCs is their high temperature which make them difficult to be used in various applications and it also puts severe constraints on the cell material [49]. They also possess high electrolyte resistivity [49]. Figure 4 shows a SOFC.

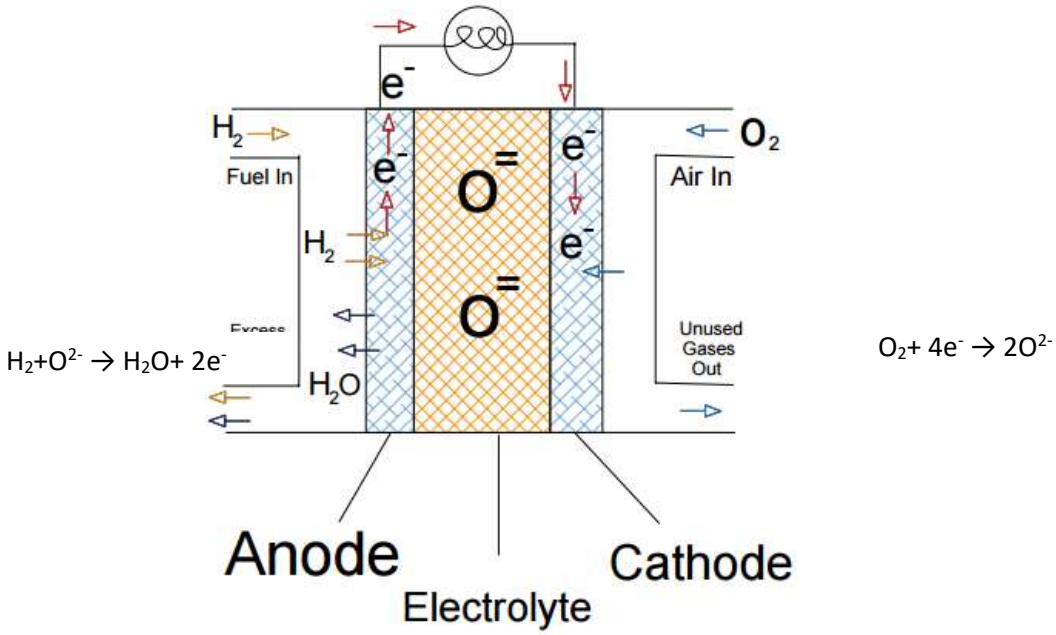

Figure 4. Solid oxide fuel cell

2.2.5. Proton exchange membranes fuel cells (PEMFCs)

Proton Exchange Membranes Fuel Cells (PEM) fuel cells are currently receiving the most interest among all other types of fuel cells. Their remarkable features such as low temperature, easy scale-up and high power density make them a promising clean and efficient power generation technology [58]. The most important application for PEM fuel cells is in the automotive industry [59]. Moreover, the light weight and the high power density make PEM fuel cells of an increasingly important for distributed cogeneration for buildings and portable powers [60]. The basic elements that make up a PEM fuel cell are bipolar plates, diffusion layers, electrodes and an electrolyte [61]. The core of the PEM fuel cells is the membrane electrode assembly (MEA) which consists of a proton exchange membrane, catalyst layers, and gas diffusion layers (GDL) [62]. The typical operating temperature for a PEM fuel cell is around 80ºC and all the materials in the cell are in the gaseous state [63]. Both the anode and cathode in PEM fuel cells are composed of platinum supported on carbon. The most commonly used fuel in PEM fuel cells is H_2 and the oxidant used is air [64].

The catalysts used in PEMFCs are: platinum, palladium, ruthenium, iridium, gold and silver [65]. Platinum (Pt) showed a superior performance over other metals, more specifically, for the oxygen reduction reaction at the fuel cell cathode [66]. Despite its superior performance, the high cost of platinum and its limited resources are

considered obstacles in the commercialization of PEM fuel cells [67]. In addition, carbon monoxide is strongly adsorbed on platinum catalyst sites in low temperatures leading to the poisoning of the precious Pt catalyst. [68]. Extensive research is going on to reduce the amount of the precious metal used or investigate new alternatives that are less expensive and efficient to replace platinum [69]. There are some disadvantages associated with PEM fuel cells including the high cost of the platinum catalyst, carbon monoxide poisoning, the slow oxygen kinetics and the limited fuel cell life [70].

Table 1 summarizes the electrolytes, operating temperature, fuels, oxidants, catalysts, and reactions of the various fuel cell types.

Table 1. Summary of fuel cell types

Type of Fuel Cells	AFC	MCFC	PAFC	SOFC	PEM
Electrolyte	KOH [78]	Molten Carbonate [38]	Phosphoric Acid [46]	Yttria stabilized ZrO_2 [75]	Ion exchange membrane [71]
Operating Temperature	Around 100°C [79]	550°C-700°C [34]	Around 200°C [44]	700°C-1000°C [50]	Around 80 [63]
Fuel	H_2 [80]	H_2/CO_2 [77]	H_2 [45]	H_2, methanol, gasoline, diesel, biogas, ethanol, syngas [56]	H_2 [63], Hydrocarbons [72]
Oxidant	Air/O_2 [80]	Air/CO_2 [77]	Air [45]	Air [75]	Air [63]
Catalyst	Nickel Alloys [81]	Nickel [35]	Platinum [47]	Perovskites [71]	Platinum [73]
Reactions	$H_2+2OH^- \rightarrow 2H_2O+2e^-$ [82] $1/2O_2 + 2H^+ +2e^- \rightarrow H_2O$ [82]	$H_2+CO_3^{2-} \rightarrow H_2O+CO_2+2e^-$ [41] $1/2O_2+ CO_2 + 2e^- \rightarrow CO_3^{2-}$ [41]	$H_2 \rightarrow 2H^+ +2e^-$ [46] $1/2O_2+ 2H^+ + 2e^- \rightarrow H_2O$ [46]	$H_2+O^{2-} \rightarrow H_2O+ 2e^-$ [76] $O_2+ 4e^- \rightarrow 2O^{2-}$ [76]	$H_2 \rightarrow 2H^+ +2e^-$ [74] $1/2O_2+2H^++2e^- \rightarrow H_2O$ [74]
Advantages	• High efficiency • Low cost • Fast kinetics	• Can be used as CCS systems • Can be coupled to gas turbines • Does not require noble metal catalysts	• High stability • Low vapor pressure • Moderate operating temperature • High tolerance for carbon dioxide	• Produce high quality heat byproducts • Do not contain noble metals • Long-life expectancy • Fuel flexibility	• Easy scale-up • High power density • All-solid structure
Disadvantages	• Intolerance to carbon dioxide	• Hardware corrosion • Low power density • Cathode dissolution	• Low power density • Intolerant to CO • Low electrolyte conductivity	• Difficult to use in various applications • High electrolyte resistivity	• high cost of platinum catalyst • Slow oxygen kinetics • limited fuel cell life • CO poisoning

2.3. Applications of Fuel Cells

2.3.1. Transportation

According to the environmental protection agency, transportation is responsible for 26% of the greenhouse emissions due to the extensive use of fossil fuels [83]. Therefore, it is very important to find an alternative power source for vehicles. The use of fuel cells in transportation is one of the most important applications for fuel cells due to their operating temperatures and planner geometry [84]. However, storing the fuel (mostly hydrogen) represents one of the main challenges in the commercialization of fuel cells. Hydrogen storage systems for example, are heavy, large and costly [85]. Moreover, hydrogen diffuses through many materials used for the storage tanks and through gaps that are usually considered small enough to safely seal other gases [85].

2.3.2. Stationary applications

Fuel cells stacks can be used as backup power generators in remote locations. They can also be used as stationary and stand-alone power plants for cities and towns or distributed generation for buildings [5]. Although PEM fuel cells are the most common type, but other types such as AFCs, PAFCs, MCFCs and SOFCs fuel cells can also be used. PEM fuel cells offer rapid startup, but as a result of the external reformer, they will have lower efficiencies than other high temperature fuel cells [86].

2.3.3. Portable applications

Fuel cells are also attractive for small portable units [75]. They can be used for many portable applications such as: remote power generation and backup solutions, auxiliary power units for cars, and demonstrators [87]. One major advantage of fuel cells over batteries for portable applications is the higher energy density it offers. Portable power packs that use fuel cells can be lighter and smaller for the same amount of energy [88]. Although the use of fuel cells in portable devices is promising, there are some challenges in using them [89]. The supply of hydrogen in electronic equipment is difficult due to storage problems. Safety is also another issue when carrying a pure hydrogen in an electrical equipment. The use of methanol as a fuel instead of hydrogen for portable systems had drawn a great attention in the recent years. However, direct methanol has the drawbacks of the low oxidation rate and the fuel crossover [89]. The diffusion of the methanol through the material of the electrolyte from the anode to the cathode causes a fuel loss of around 40% [90].

2.4. Direct Hydrocarbon Fuel Cells

2.4.1. Rational for using direct hydrocarbons in fuel cells

Fuel cells can be further categorized based on the fuel used, to hydrogen, direct hydrocarbon and methanol fuel cells. Hydrogen is the major fuel in all types of fuel cells as it gives the highest current density among all other types of fuels [14]. However, hydrogen is not readily available. It also has a much lower energy storage density as opposed to other hydrocarbons. Hydrogen flammability is problematic as it can ignite in low concentrations and leak through seals [91]. Most hydrogen is currently produced by steam reforming of natural gas followed by the water gas shift reaction [92]. This process emits carbon dioxide (CO_2) as a product.

Methanol is the second most widely used fuel in PEMFCs. Methanol is highly toxic, emits formaldehydes to the air, very corrosive and requires a special fuel handling system which will increase the capital cost [91]. The slow kinetics at the anode and the crossover of methanol through the membranes are two main problems that cause the efficiency of direct methanol fuel cells to decrease [93].

In this project, hydrocarbons, such as propane, are proposed as fuels for PEMFCs. Hydrocarbon fuel can directly be fed at the fuel cell anode and go through an electro-oxidation reaction. The use of hydrocarbons as fuel has the potential to solve many of the problems associated with the use of hydrogen and methanol since they are less expensive, more readily available and more safely stored [94].

Direct hydrocarbon fuel cells (DHFCs) were extensively studied in the 1960s [19]. The cost-per-kWh delivered from hydrogen generated from fossil fuels is much higher than the cost-per-kWh when using a fuel directly in the fuel cell [95]. Furthermore, the most common way for producing hydrogen is by using an external reformer. In the external reformer, the fuel catalytically reacts with oxygen or water to form a mixture of H_2, CO, CO_2, N_2, and H_2O which increases the complexity and the cost of the fuel cell system [94]. The fuel supply, storage subsystems and other hydrogen production equipment constitute about half the cost of the fuel cell system [95]. Therefore, eliminating the fuel processor unit will significantly drop the cost of the fuel cell system. The fuel processor unit also causes inevitable amounts of CO_2 emissions which lead to greenhouse effects [96]. The average CO_2 emission from a methane steam reformer, which is the main hydrogen production process, is 7 kg

CO_2/kg H_2 [97]. If hydrocarbons are directly fed into the anode, the CO_2 emissions will significantly drop. Taking propane as an example, the average CO_2 emission is 3 kg CO_2/kg C_3H_8.

2.4.2. Types of direct hydrocarbon fuel cells

2.4.2.1. Hydrocarbon fuels in phosphoric acid fuel cells

In the 1960s, phosphoric acid fuel cells were the first and most frequent fuel cells to be investigated for the use with direct hydrocarbon fuels. The temperature range at which the direct hydrocarbon phosphoric acid fuel cells were investigated was between 150 and 200 ºC. In 1983, Pratt and Whitney had developed a 250-400 kW phosphoric acid fuel cell that produces stationary electric power at which 300 units were constructed in 19 countries [98].

Several acids including KOH, HF and H_3PO_4 were investigated as electrolytes in direct hydrocarbons fuel cells. KOH have the tendency to react with CO_2 which results from the hydrocarbons oxidation. This leads to K_2CO_3 formation and HF. This mixture forms an azeotrope with water at a maximum boiling temperature of 120ºC [99]. Therefore, the most practical acid to be chosen as an electrolyte for direct hydrocarbon fuel cells is H_3PO_4.

One of the major advantages of having H_3PO_4 as an electrolyte in direct hydrocarbon fuel cells is overcoming the cycling phenomenon that direct hydrocarbon fuel cells exhibit at certain conditions. With each cycle, the adsorbed species will accumulate on the electrode causing the effective surface area to decease and hence decreasing the rate of the electrode reaction [99]. In case of phosphoric acid electrolyte, the cycling is tolerable when the fuel used is propane [99].

Several hydrocarbons fuels were studied in phosphoric acid fuel cells. Among the other hydrocarbons, propane gave the highest oxidation rate [99] . In 2015, Zhu et al. have examined a direct n-hexadecane phosphoric acid fuel cell [98]. The anodic half reaction is as follows:

$$C_{16}H_{34} + 32\ H_2O \rightarrow 16\ CO_2 + 98\ H^+ + 98\ e^- \quad (2.1)$$

The cathodic reaction is:

$$49/2\ O_2 + 98\ H^+ + 98\ e^- \rightarrow 49\ H_2O \quad (2.2)$$

Therefore, the overall equation is represented as follows:

$$C_{16}H_{34} + 49/2\ O_2 \rightarrow 16\ CO_2 + 17\ H_2O \quad (2.3)$$

The electrolyte in the study was phosphoric acid, and the catalyst for both the anode and the cathode was Pt supported on carbon [98]. The experiment was conducted at two different temperatures; 160^{o}C and 190^{o}C. The results showed a deactivation characterized by the potential decrease over time. This deactivation was attributed to the formation of either CO_2 or carbonaceous deposits [98]. In this described system, since the temperature was low, the reforming reaction was unfavorable. In order to increase the current density, it was concluded that a large reactor with higher capital cost is required [98].

2.4.2.2. Hydrocarbon fuels in solid oxide fuel cells

Due to their high operating temperature, SOFCs have the potential to operate with direct hydrocarbons without the need for an external reformer and this reduces the overall cost of the system [100]. The high operating temperature gives SOFCs the advantage of being tolerant to a wide range of fuels. For instance, CO, which is considered to be poisonous for low-temperature fuel cells, is a fuel for SOFCs [101]. One of the main methods for the feeding of hydrocarbons in SOFCs is the internal reforming of hydrocarbons which is given by the following equation [102]:

$$C_nH_{2n+2} + nH_2O \rightarrow nC + (2n+1)H_2 \quad (2.4)$$

Internal has some disadvantages that prevents its commercialization [102]. The internal reforming requires a significant amount of water in the fuel which causes the fuel to be diluted and hence reducing the electromotive force of the cell [103]. In addition, the steam reforming is an endothermic process that causes a strong cooling in the inlet area of the stack and results in a large temperature gradient [104]. Due to the limitations of internal reforming, the primary technology that attracts the attention is the direct feeding of hydrocarbons with a minimal amount of water and oxygen. The direct oxidation or utilization of hydrocarbons in SOFCs is given by the following equation:

$$C_nH_{2n+2} + (3n + 1)\ O^{2-} \rightarrow nCO_2 + (n + 1)\ H_2O + (6n + 2)\ e^{-} \quad (2.5)$$

One of the most important issues associated with the use of direct hydrocarbons in SOFCs is fouling which is caused by the deposition of carbon. When the temperature of the SOFC is high, the hydrocarbons will react on the surface of the anode forming tars that will be deposited on the anode resulting in a significant drop in the stability of the cell [105]. Since the conventional Ni based anodes have problem of carbon deposition (coking) and deactivation in the hydrocarbon fuel, alternative anodes have been developed such as Cu-based cermet, and doped $(La,Sr)(Ti)O_3$ [106]. These alternative anodes showed an improvement in coking tolerance for light hydrocarbons. However, they have a low conductivity, low physical, chemical, and thermal compatibility with YSZ electrolyte at high temperatures and poor electrochemical activity [106].

Despite the problem of carbon formation and coking, Ni-YSZ is yet one of the most conventional anode choices for SOFCs. Ni is not only a good conductor but also a good electrocatalyst for H_2 and CO reactions above 600 ^oC [76]. Therefore, to maintain high performance of SOFC operated with direct hydrocarbon fuel with Ni-based anodes while eliminating the chance of coking, a thin catalytic coating can be applied to the Ni anodes [106]. The thin catalytic coats include SDC, Sn and BaO which promote the hydrocarbons before reaching the Ni anode and thus enhancing the coking tolerance [106]. Another anode that is used in SOFCs operated with direct hydrocarbon fuel cells, and proved to be effective, is Cu-ceria-YSZ [105]. The use of Cu-ceria-YSZ significantly reduces the carbon formation issue and at the same times gives an excellent performance [105].

Sulfur imposes another problem in operating hydrocarbons in SOFC. Fuel cells are very sensitive to sulfur since it will react with the anode materials and produce sulfur containing compounds [105]. The problem can be eliminated if the produced compounds are stable. For instance, when sulfur reacts with Cu-ceria-YSZ anodes, Ce_2O_2S is formed and it is relatively stable [105].

Butane, nethane, ethane, ethylene, iso-octane, propane-1,2,3-triol, dimethoxymethane, ethoxyethane, and trimethoxymethane can be directly fed into SOFC. The conversion in SOFC using direct hydrocarbons increases as the temperature increases [76]. Dean et al. conducted a study using butane as a fuel, it was observed that a full conversion was achieved at 800^oC whereas no conversion occurred below

550ºC [76]. In one experiment testing various hydrocarbons including n-decane, toluene and fuel gas, under the same conditions, the power densities obtained were all identical [105].

As can be concluded from this section, although more research is still a necessity for the commercialization of SOFCs that operates with direct hydrocarbons, it can clearly be seen that they have a huge potential to be used as energy sources in many areas including electrical generators [107].

2.4.2.3. Hydrocarbon fuels in Proton Exchange Membrane fuel cells (PEMFCs)

PEM fuel cells have attracted a huge attention for the several advantages including high power density and all solid cell compartments [108]. Hydrogen is still the number one choice when it comes to PEMFC fuels selection, due to its high performance. Hydrocarbons offer an alternative fuel choice and they can either be fed directly to the cell or converted to hydrogen using an external reformer. The latter however has problems of complexity and extra cost added to the fuel cell system [94]. A considerable amount of research was done in the 1960s on the direct hydrocarbon PEM fuel cells (DH PEMFC). The properties of hydrocarbons made them attractive to be used in PEM fuel cells. Propane for instance, is cheap, can be stored in the liquid form is pressurized vessels and has a high-power density [109].

The electro-oxidation reactions in direct hydrocarbon PEM fuel cells were studied on platinum (Pt) and palladium. Platinum (Pt) gave better results [109]. An extensive research was performed on the direct hydrocarbon fuel cells using variety of hydrocarbons such as normal paraffins, olefins, gasoline and diesel [110]. The research results showed very low cell potential when normal alkanes were used [110].

The performance of hydrocarbon fuels was addresses in the literature by several studies. In 1996, a group of researchers at University of California built a direct hydrocarbon PEMFC that was operated with propane and based on the design of the Los Alamos National Laboratory (LANL). The fuel cell was completely covered with Teflon to eliminate any gas leak. [111]. The electrolyte in this study was Nafion, the anode was Pt and the cathode was based on gold-lead [111]. The testing temperature of the cell was 50 ºC. The experimental results showed a poor electro-catalytic activity [111]. It was then proposed to operate the cell at a temperature higher than 100 ºC in

order to speed up the electro-chemical reaction kinetics [111]. The anode performance in a direct hydrocarbon fuel cell was studied using different hydrocarbons; butane, ethane, n-butane, methane, ethylene, propylene, and iso-butylene. The highest performance, which is measured by activity per unit surface area of electrocatalyst, was obtained with propane and the lowest was with methane, ethylene, propylene, and iso-butylene [111].

Savadogo and Rodriguez Varela [109], have worked on low-temperature direct propane polymer electrolyte membranes fuel cells. The membranes in their study were Nafion 117 doped with heteropolyacids (HPAs) and polybenzimidazole (PBI) doped with acid. The results of this study may be summarized as follows: direct propane fuel cells are cheaper and have greater temperature ranges compared to methanol fuel cells, the handling and infrastructure of direct propane fuel cells are easy and they have the potential to work with low cost membranes that can replace Nafion [109].

2.5. PEM Fuel Cell Efficiency

The efficiency of a fuel cell is determined by the ratio of work out/heat in. The maximum amount of "work out" or the useful amount available in the system to do work at constant pressure and temperature is the Gibbs free energy, ΔG_f. The amount of heat in is the "enthalpy of formation", ΔH_f or the amount that would be produced by burning the fuel. Thus, the efficiency of the fuel cell is equal to $\Delta G/\Delta H$ for a certain fuel/oxidant reaction.

At standard conditions, the free energy of water formation is [102]:

$H_2 + ½\ O_2 \rightarrow H_2O_{(l)}$ $\Delta H_f = -285.84$ kJ/mol

The free energy available for useful work is -237.3 kJ/mol [102]. Therefore, the thermal efficiency of a fuel cell operating on pure hydrogen and oxygen at standard conditions is:

$$\eta = \frac{237.3}{285.84} x\ 100 = 83\%$$

Taking a hydrocarbon fuel as an example, i.e. propane C_3H_8, then based on the following reactions:

- Anode: $C_3H_8 + 6H_2O \rightarrow 3CO_2 + 20e^- + 20H^+$ $E_o = 0.137$ V (2.6)
- Cathode: $5O_2 + 20e^- + 20H^+ \rightarrow 10\ H_2O$ $E_o = 1.229$ V (2.7)

- Overall: $C_3H_8 + 5O_2 \rightarrow 3CO_2 + 4H_2O$ $E_{cell} = 1.092$ V (2.8)

The values of $\Delta G = -2107$ kJ and $\Delta H = -2219$ kJ, hence, the fuel cell efficiency is calculated as follows [112]:

$$\eta = \frac{\Delta G}{\Delta H} = \frac{-2107}{-2219} = 0.95$$

As can be seen, direct hydrocarbon fuel cells have a theoretical efficiency of 95% and an actual efficiency of 32% whereas hydrogen fuel cells have a theoretical efficiency of 83% and an actual efficiency of 32% [14]. This implies that direct hydrocarbon fuel cells have a much greater room for improvement than hydrogen fuel cells. One of the important areas to be improved in order to enhance the efficiency of direct hydrocarbon PEMFC is the electrocatalyst surfaces of the anode electrodes [14]. This can be accomplished by operating at higher temperatures to speed up the reaction kinetics.

2.6. Motivation for High Temperature Operation

The previous context shows that the main problem associated with DHFCs is their low reaction rates (low current density). The maximum oxidation current density attained from PEM fuel cell operated with propane with Pt electrode was reported to be less than 2 mA/cm^2 at 0.2 V [109]. Moreover, the operation at low temperature leads to low electro-catalytic activity and poor anode stability. However, the theoretical energy efficiency for a direct hydrocarbon fuel cell is higher than that of hydrogen. Hence, it appears that there is a merit toward using a hydrocarbon fuel but the electro-catalytic activity of the cell should be improved. High temperature operation improves the cell tolerance for CO impurities, hence, allowing the use of a wider range of fuels. Small amounts of CO as low as 10 ppm [17] can poison the catalyst. It has been shown that the CO coverage on the catalyst surface can be reduced by increasing the temperature [113]. A study was performed on the platinum based catalysts and showed that these can tolerate up to 1000 ppm CO at 130°C [114].

High temperature operation also allows the generation and the recovery of useful heat and reduces the problems associated with liquid water accumulation at the cathode. The reduction of liquid water content will assist in increasing the exposed surface area of the catalyst allowing more molecules to diffuse into the reaction sites.

All these reasons are incentives for working at higher temperatures. Nafion and similar PEM's membranes have limited possibilities of fulfilling this target because proton conduction is dependent on the hydration levels in these membranes and Nafion loses its conductivity due to water loss (dehydration). For example, Nafion conductivity decreases from 0.066 to 0.00014 S cm^{-1} at 30°C when the relative humidity (RH) decreases from 100% to 34% [17]. Furthermore, the low glass transition temperature of Nafion (110 °C) is problematic because above this point the polymer loses its mechanical stability and degradation eventually occurs [115].

2.7. Thermodynamics of PEM Fuel Cells

McIntosh and Gorte [105], calculated the Nernst potential for H_2 and for a hydrocarbon (n-butane). They studied the effect of conversion on the equilibrium potential for both fuels. It was found that when hydrogen is used, the potential drops by 15% between 10 and 80% conversion [105]. However, when hydrocarbons are used, the potential drops only by 1% over the same conversion range for n-butane [105].

The performance of a fuel cell is evaluated through a plot called a polarization curve. The potential of the fuel cell in volts is drawn versus the current density (mA/cm^2) as shown in Figure 5. This figure shows a typical polarization curve. It is expected that the cell potential would be equal to the thermodynamic value (e.g. V= 1.092 V for propane) with increasing reaction rates or current densities. However, the polarization curve shows a drop in potential as the current density of the fuel cell increases. This curve could be divided into three regions: 1) activation, 2) Ohmic and 3) concentration. The polarization curve shows a drop in potential as the current density of the fuel cell increases. This is due to various phenomena taking places inside the fuel cell on the electrodes, the membrane and the inner components in general. The potential of a fuel cell is basically deviating from the equilibrium value. In the first region, the activation polarization, a drop in potential is observed to be surface phenomena taking place on the electrodes surface and attributed to surface diffusion, reaction and, desorption. In principle, the activation polarization is only dominant at low current density due to the electronic barriers that are needed to be overcome before the ion and current flow. It is primarily influenced by the electrochemical reaction rate at which the fuel and oxidant are being oxidized or reduced [102].

The second region in the curve is the Ohmic polarization. Further drop in potential is observed. This is the result of the resistance to the flow of protons in the electrolyte (membrane) and electrons in the cell components and external wires. The ohmic polarization can be expressed by Ohm's law as follows [95]: $E_o = i (R_{ele} + R_{ion} + R_{CR})$, where R_{ele}, R_{ion}, R_{CR} are the electronic, ionic and contact resistances in Ω cm^2. Several ways are used to reduce the ohmic losses such as using electrodes with very high conductivities, reducing the distance that the electrons need to travel and creating thin electrodes in order to give the protons a shorter distance to travel [5].

The third region is concentration polarization. At this point the fuel cell potential further drops due to mass transfer limitations. One example in a PEMFC is the accumulation of water at the cathode, imposing more resistance to the diffusion of oxygen to the catalyst sites. This resistance becomes very large when liquid water floods the pore structure of the cathode catalyst in the PEMFC. Figure 5 shows a typical polarization curve for a PEMFC with hydrogen as a fuel as an illustration.

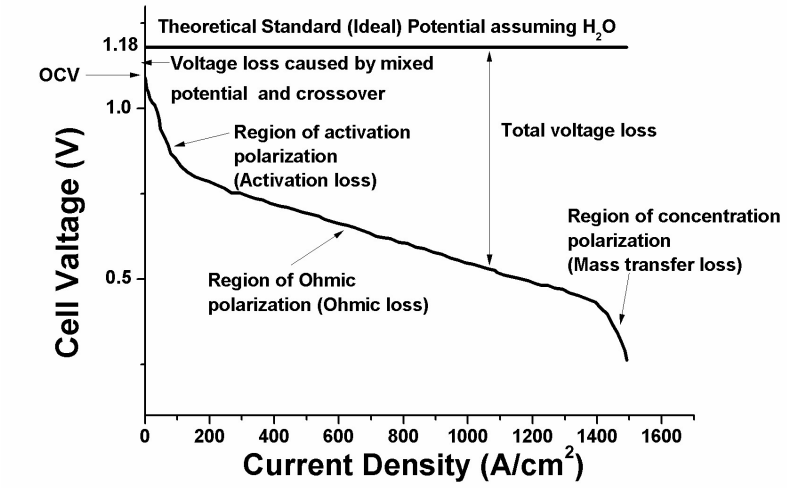

Figure 5. Polarization curve for a typical fuel cell [116]

2.8. PEM Fuel Cells Membranes

Membranes based on perfluorosulfonic acid such as Nafion, are the most successful in PEM fuel cells. Nafion was developed by DuPont in the 1960s [117]. The perfluorinated composition of the membrane provides the thermal and chemical stability, whereas sulfonation makes it a hydrophilic material, thus, enhancing its water content. The fuel cell membrane is a proton conducting material. Protons transport in

the membrane is known to occur via the hopping mechanism on water molecules [118]. Hence, water content is essential in Nafion to ensure reasonable proton conductivity. Nafion's proton conductivity significantly decreases if the temperature is increased beyond 80^{o}C due to dehydration [60]. Therefore, it can be concluded that Nafion cannot be used for high temperature applications. Instead, research efforts are directed toward improving the existing Perfluorosulfonic acid or developing alternatives for Nafion to be used in high temperature fuel cells applications. Many approaches have been followed in the literature. One of these approaches was to use solid proton conductors such as zirconium phosphates.

2.8.1. Zirconium hydrogen phosphate

Zirconium hydrogen phosphate $Zr(HPO_4)_2$ or ZrP is a solid proton conductor [21]. The cation exchange behavior of ZrP was discovered in the 1950s and since then, there has been a huge interest in it. The ion exchange properties of ZrP are due to its layered structure which allows the passage of guest molecules and the weak acidic groups which allows the protons in the POH group to be exchanged with other cations and anions [22]. The mobility of the surface protons is much higher than the mobility of the internal ones [119]. Therefore, the surface protons cause high proton conductivity.

An extensive study on ZrP was reported in 1958 by Amphlett [120]. It was shown that ZrP is one of the most stable inorganic hydrogen exchangers and it can be refluxed in water for weeks without any noticeable breakdown [120]. ZrP is formed by a precipitation of a soluble zirconyl salt with phosphoric acid. Each Zirconium atom (Zr) is attached to number of phosphate groups [121]. The precipitation reaction of ZrP proceeds according to the following reaction:

$$ZrOCl_2 + 2H_3PO_4 \rightarrow Zr(HPO_4)_2 + 2HCl + H_2O \quad (2.9)$$

The specific conductance of ZrP was studied by Alberti et al. in 1978 [122]. It was indicated that its specific conductance decreases with the increase in the degree of crystallinity due to the decrease in the total number of defects. It was also shown that the mobility of the surface ions (responsible for proton conductivity) was 10^4 times higher than the core ions [122]. In the 1960s, the crystalline form of ZrP ($Zr(HPO_4)_2 . H_2O$) was prepared and that further enhanced its ion exchange properties. ZrP was successfully incorporated into perfluorinated sulfonic acid membranes in the 1990s by

Grot and Rajendran [123]. The incorporation was done by an exchange precipitation process [123]. ZrP is a hydrophilic, inorganic compound, and its presence in the membrane creates an additional pathway for the proton conduction inside the membrane [20]. It also reduces the water loss as the temperature increases owing to the hydrogen bond within the chemical structure, hence, the proton conductivity of the membrane is increased [123]. ZrP possessed reasonable proton conductivities at temperatures up to 300ºC [124]. ZrP was successfully incorporated in Nafion [125]. The Nafion/α-ZrP composite membrane had a conductivity of 0.1 S cm^{-1} at 373 K and 100 Relative Humidity (RH). The reported proton conductivity for ZrP was in the range of 10^{-7} – 10^{-5} S cm^{-1} [126, 127, 128].

2.8.2. Effect of ionic liquids

Ionic liquids are salts which are liquid at, or near, room temperature, and are composed of organic cations and inorganic anions [129]. The number of possible ionic liquids is almost unlimited due to the large number of possible combinations between anions and cations. For this reason, they are regarded as designer solvents [130]. Many ionic liquids have attractive properties such as negligible vapor pressure, non-flammability, high ionic conductivity and thermal stability over a wide temperature range [131, 132]. These properties make ionic liquids very attractive in the electrochemistry field. Ionic liquids can be used in several electrochemical energy applications including high energy density batteries, solar cells and fuel cells [133]. Recently, significant work is directed toward the use of ionic liquids in high temperature PEM fuel cells membranes due to their high thermal stability. As of a result of the acid-base nature of ionic liquids and their capability for hydrogen bonding, they have the ability to transport protons [134].

The interesting characteristics that are demonstrated by ionic liquids make them suitable for incorporation in PEM fuel cell membranes [135]. 1-Butyl-3-methylimidazolium trifluoromethane sulfonate was incorporated within Nafion membrane. The measured ionic conductivity of the composite membrane was 0.1 S cm^{-1} at 180ºC [136]. This promising increase in the ionic conductivity had attracted a huge attention to the use of ionic liquids in fuel cell membranes. 1-Butyl-3-methylimidazolium tetrafluoroborate was incorporated in sulfonated poly ether ether ketone polymer (SPEEK) with a proton conductivity of 0.01 S cm^{-1} [137]. Ionic liquids were used as solvents to prepare ZrP using the ionothermal method in two studies;

Smeets [138] and Gui [139]. No data about the proton conductivity was reported in Smeets et.al study. Gui et al. prepared a layered ZrP material in a solvent of 1-ethyl- 3-methylimidazolium hexafluorophosphate. The proton conductivities were 0.0145 S cm^{-1}(at 363 K, 95% relative humidity) and 1.1×10^{-5} S cm^{-1} at 503 K [139].

Ionic liquids can be divided into hydrophilic and hydrophobic. In this project, the effect of a range of ionic liquids on the proton conductivity of the PEMFC membrane is tested. For example, hydrophilic ionic liquids such as 1-ethyl-3-methylimidazolium ethyl sulfate, 1-butyl-3-methylimidazolium dicyanamide, and 1-butyl-3-methylimidazolium triflate were investigated. These ionic liquids contain the hydrophilic anions and were expected to increase the water content inside the membrane; hence it was anticipated that they will enhance the proton conductivity.

2.8.3. Effect of Glycerol

The effect of glycerol on the morphology and conductivity of composite a ZrP/PTFE membrane for a PEM fuel cell, processed at 200ºC, was reported in 2012 [140]. It was found that the addition of glycerol enhanced the proton conductivity of the membrane. Glycerol changed the morphology of the ZrP particles from flakes with more than 1 μm diameter to a nearly sphere shaped particles with diameter of 100–500 nm [140]. This has given a greater surface area for the transport of protons. Moreover, the proton transport, after the addition of glycerol, is caused by a combination of the OH groups in both the ZrP bulk and the glycerol [140]. As a result, the proton conductivity showed a substantial increase. The proton conductivity of GLY/ZrP/PTFE composite membrane was measured as 0.02–0.045 S cm^{-1} compared to 10^{-3} S cm^{-1} in the absence of glycerol [140].

Chapter 3. Experimental Work

3.1. Introduction

In this work, a group of hydrophilic ionic liquids were incorporated in zirconium phosphates then investigated for their proton conducting properties. The ionic liquids were added to a solution of $ZrOCl_2$, followed by a precipitation reaction with H_3PO_4 to prepare the ZrP/IL modified materials. The synthesized materials were evaluated for proton conducting properties, thermal stability, morphology and structure via different techniques including electrochemical impedance spectroscopy (EIS), thermogravimetric analysis (TGA), scanning electron microscopy (SEM), X-ray diffraction (XRD), Fourier transform infrared spectroscopy (FTIR) and Raman spectroscopy.

3.2. Materials

3.2.1. Zirconium oxychloride ($ZrOCl_2$)

The $ZrOCl_2$ used in this research was ACS 98% purity, reagent grade, and purchased from SIGMA ALDRICH.

3.2.2. Phosphoric Acid

The phosphoric acid used in this study was 85% purity by weight, assay grade.

3.2.3. Ionic liquids

All ionic liquids were purchased from IoLiTec GmbH. The ionic liquids were used without further purification.

1- 1-butyl-3-Methylimidazolium triflate, 99% purity
2- 1-ethyl-3-methylimidazolium ethyl sulfate, 99% purity
3- 1-ethyl-3-methylimidazolium acetate, >95% purity
4- 1-ethyl-3-methylimidazolium trifluoroacetate, >97% purity
5- diethylmethylammonium methanesulfonate >98% purity
6- 1-butyl-3-methylimidazolium dicyanamide, >98% purity
7- diethylmethylammonium trifluoromethanesulfonate, >98% purity

3.3. Preparation of Zirconium Phosphate/ Ionic Liquid Powder Samples (ZrP/IL)

ZrP/IL samples were prepared by mixing aqueous zirconium oxychloride solution ($ZrOCl_2$) with 85% phosphoric acid (H_3PO_4), in the presence of ionic liquids, according to the following reaction, at room temperature:

$$ZrOCl_2(aq) + 2H_3PO_4 \rightarrow Zr(HPO_4)_2 + 2HCl + H_2O \quad (3.1)$$

100 mL of 0.19 M of $ZrOCl_2$ was prepared using $ZrOCl_2 \cdot 8H_2O$. Ionic liquids were added to the $ZrOCl_2$ solution, prior to the reaction, in mass percentages ranging between 0.4 and 5%. The gel resulting from the reaction was filtered and washed with distilled water and ethanol in a 2:1 volume ratio. The filtered gel was then dried in the oven at 60 ^oC for 2.5 hours and then left to dry at room temperature for 72 h.

3.4. Characterization of the Synthesized ZrP/IL Material

The ZrP/IL materials synthesized in this work were subjected to the following characterization techniques:

3.4.1. Electrochemical impedance spectroscopy (EIS)

Electrochemical impedance spectroscopy (EIS) was used to measure the proton conductivity of the ZrP/IL material as this is one of the main objectives of this study. EIS works by applying a certain alternating potential and the alternating current response is analyzed and presented in a typical plot called Nyquist plot. The electrochemical impedance of the ZrP/IL samples, in this study, was measured using the four-probe measurement method. Approximately 0.2 g of the ZrP/IL sample was placed in an electrochemical cell with stainless steel electrodes. The cell was connected to a potentiostat (BioLogic, SP-200). The EIS tests were performed at a frequency of 0.0001-200 kHz. The response was reported in Nyquist plot. The value of the sample resistance value R (Ω) was obtained by the intersection of the graph with the x-axis at the high frequency region. The resistance (R) was then used to calculate the conductivity of the samples using equation 3.2.

$$\sigma = \frac{t}{R * A} \quad (3.2)$$

In this equation, t is the thickness of the sample in cm, A is the area of the cell in cm^2 and R is the impedance of the sample in Ω.

3.4.2. Thermogravimetric analysis (TGA)

Thermogravimetric analysis (TGA) was used in this work to investigate the thermal stability of the synthesized ZrP/IL materials and the pure ionic liquid [EMIM][ESO_4], and monitor the water loss as a function of temperature. The water content of the samples is important in studying the proton conductivity as increasing the water content of the material, increases its proton conductivity. The TGA analysis was performed using PerkinElmer, TGA 4000 Thermogravimetric Analyzer. The samples were heated from 35^oC to 925^oC at a heating rate of 10^oC/min, in N_2 atmosphere with a flow rate of 20 mL/min. The TGA and DTG curves of the synthesized materials were compared to that of the pure ZrP sample.

3.4.3. X-Ray diffraction (XRD)

X-ray diffraction (XRD) was used to analyze the structure of the ZrP/IL materials and to study the ZrP-IL interaction by calculating the d-spacing of the produced ZrP material. A change in the d-spacing will give an indication of ionic liquids intercalation within the layers of the ZrP materials which will help in understanding the nature of interaction between ionic liquids and the ZrP. The XRD analysis was performed using Bruker D8 Advance, scintillation point detector and 1-D detector.

3.4.4. Fourier transform infrared spectroscopy (FTIR)

Fourier transform infrared spectroscopy (FTIR) analysis (PerkinElmer, Spectrum One FT-IR Spectrometer, wavelength range of 7,800 – 350 cm^{-1}) was used to study the surface chemistry and determine the chemical interactions in the ZrP/IL materials and compare them with the bonds in the pure ZrP material.

3.4.5. Scanning electron microscopy (SEM)

Scanning electron microscopy (SEM) was used to investigate the morphology changes of the ZrP/IL materials. SEM was done using Tescan VEGA XMU, LaB6 filament, Oxford Instruments X-Max 50 SSD detector. The SEM images of the synthesized materials were compared to the images of the pure ZrP material.

3.4.6. Raman Spectroscopy

Raman spectroscopy (Renishaw InVia Raman Spectrometer) was performed to identify the main molecular vibrations in the pure ZrP and modified ZrP/IL materials in order to identify the main functional groups present in the samples.

Chapter 4. Results and Discussion – Ionic Liquids

4.1. Introduction

In the present study, seven ionic liquids were incorporated within ZrP material. Each ionic liquid was added in mass percentages ranging between 0.4% and 5%. With each ionic liquid, the highest conductivity was reached at a certain mass percentage. Based on the conductivity measurements, the three ionic liquids with the highest conductivity were chosen for further analysis.

The main purpose of this study was to develop a material with high proton conductivity for PEM fuel cells, that can have a reasonable proton conductivity at high temperatures. The ionic liquids chosen were all hydrophilic to enhance the water content of the ZrP material, which is anticipated to enhance the proton conductivity.

Table 2 summarizes some of the physical properties of the ionic liquids studied in this work. Their chemical structure is shown in Figure 6.

Table 2. Physical properties of the tested ionic liquids at 25ºC

Ionic Liquid	Hydrophilic/Hydrophobic	Protic/Aprotic	Viscosity (Pa . S)	Electrical Conductivity (S cm^{-1})
[EMIM][ESO_4]	Hydrophilic	Aprotic	0.0959 [141]	0.38 [141]
[BMIM][DCA]	Hydrophilic	Aprotic	0.0301 [142]	1.052 [143]
[BMIM] [OTF]	Hydrophilic	Aprotic	0.0991 [142]	0.29 [143]
[EMIM][AC]	Hydrophilic	Aprotic	0.141 [144]	0.295 [141]
[BMIM] [TFA]	Hydrophilic	Aprotic	0.032 [145]	-
[DEMA][OMS]	Hydrophilic	Protic	-	6.2×10^{-3} (40ºC) [146]
[DEMA][OTF]	Hydrophilic	Protic	0.0369 [147]	0.833 (30ºC) [147]

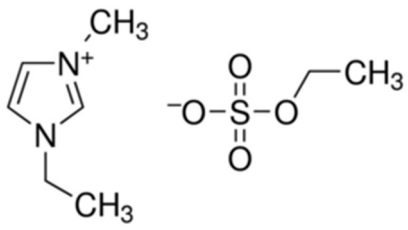

[EMIM][ESO4]

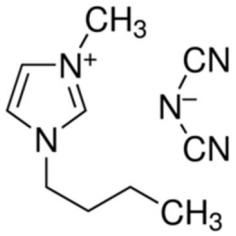

[BMIM][DCA]

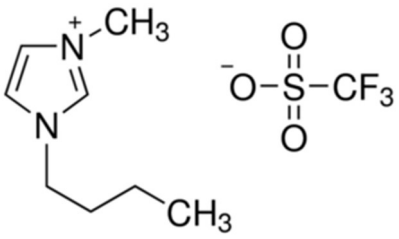

[BMIM] [OTF]

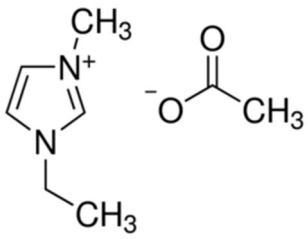

[EMIM][AC]

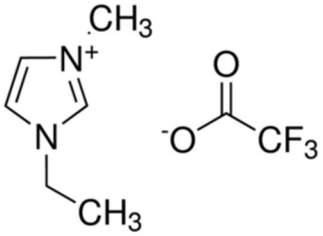

[BMIM] [TFA]

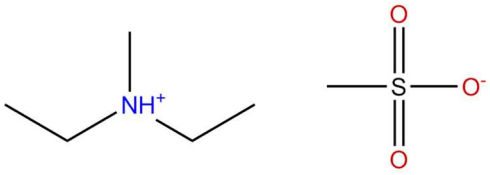

[DEMA][OMS]

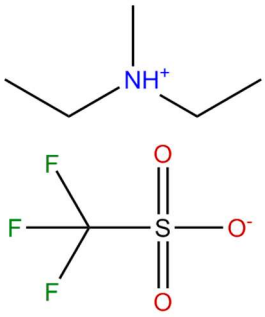

[DEMA][OTF]

Figure 6. Chemical structure of the tested ionic liquids [148, 149].

4.2. Conductivity measurements

The proton conductivity values of all the ZrP/IL samples including the best conducting samples are summarized in Table 3.

Table 3. Conductivity values for the ZrP and ZrP/IL samples

Sample	Optimum IL mass percentage (%)	Conductivity (S cm^{-1})
ZrP (No IL) (this work)	-	9.24×10^{-4}
ZrP/[EMIM][ESO_4]	0.8	2.26×10^{-2}
ZrP/[BMIM][DCA]	0.8	1.36×10^{-2}
ZrP/[BMIM] [OTF]	3	1.61×10^{-2}
ZrP/[EMIM][AC]	2.8	2.84×10^{-3}
ZrP/[BMIM] [TFA]	1.8	3.40×10^{-3}
ZrP/[DEMA][OMS]	2	4.13×10^{-3}
[DEMA][OTF]	3	2.23×10^{-3}

As shown in Table 3, among all the ionic liquids tested, 1-ethyl-3-methylimidazolium ethyl sulfate ([EMIM][ESO_4]) ,1-butyl-3-methylimidazolium dicyanamide ([BMIM][DCA]), and 1-butyl-3-methylimidazolium triflate ([BMIM] [OTF]) produced the best conductivity values. These three ionic liquids were the ones chosen for further investigation.

Electrochemical impedance spectroscopy (EIS) analyses (Nyquist Plots) were performed on the modified ZrP/IL material. The EIS spectra for the best three conducting ZrP/IL samples and the pure ZrP material are shown in Figure 7 and Figure 8. The sample resistance of the ZrP/IL materials was found from the extrapolation of the EIS spectra at the high frequency range to find their intercept with the x-axis. It can be seen that the EIS pattern is characterized by a semi-circle, which indicates a kinetic controlled process, except for the ZrP/[EMIM][ESO_4] that results in a straight line. The straight line is called Warburg line and indicates a diffusion controlled process. The proton conductivity was then calculated based on Eq. 3.2.

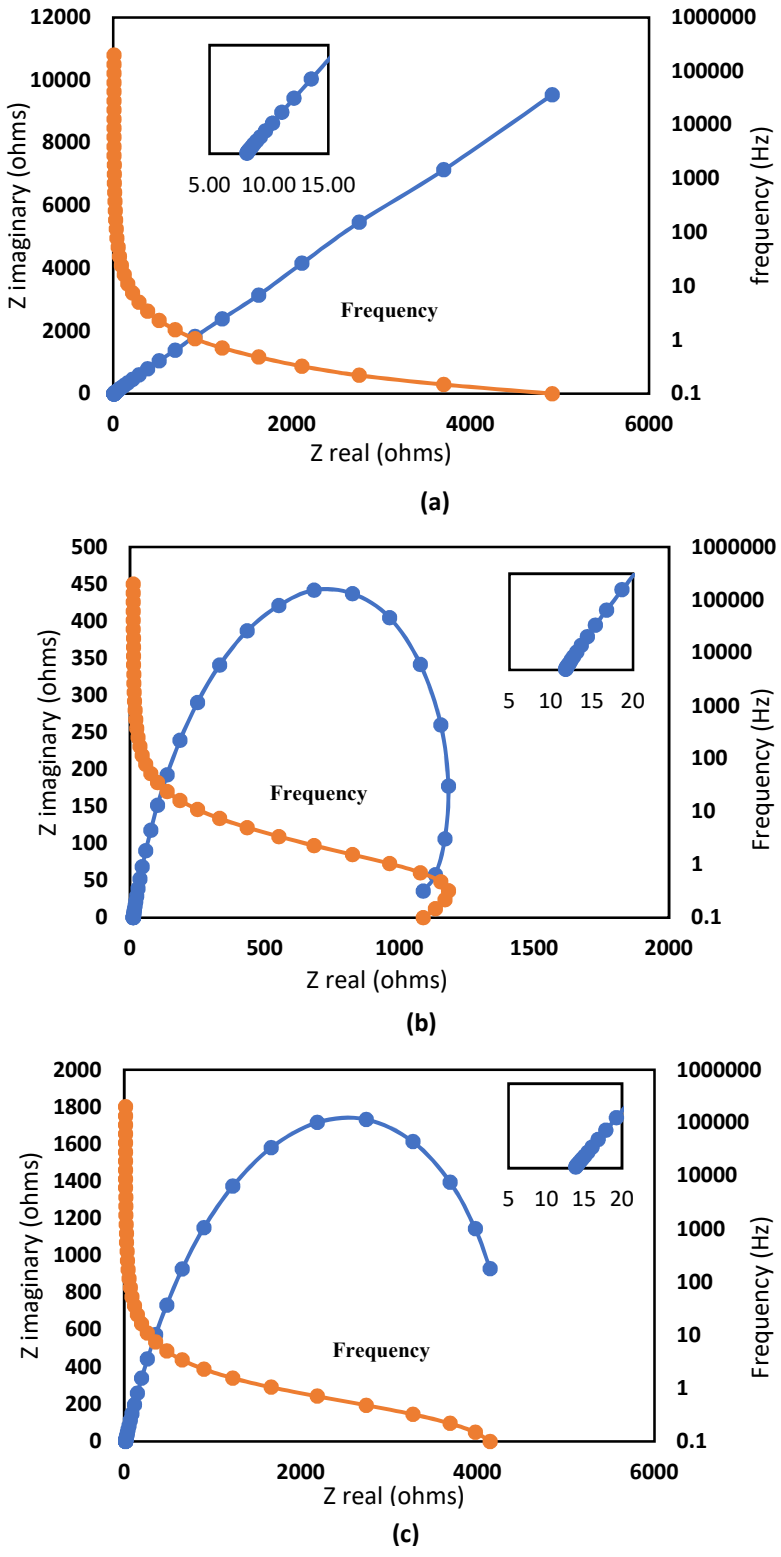

Figure 7. Nyquist plot for the modified ZrP materials. (a) ZrP/[EMIM][ESO_4], (b) ZrP/[BMIM][DCA] and (c) ZrP/[BMIM] [OTF] with zoom-in for the x-axis intercept for Z real vs. Z imaginary. Z real represents the real impedance and Z imaginary represent the imaginary impedance.

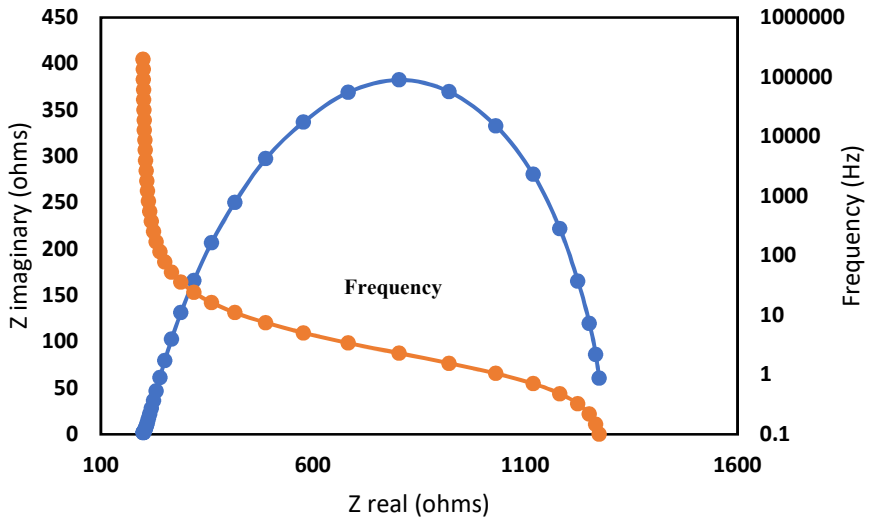

Figure 8. Nyquist plot for pure ZrP sample. Z real represents the real impedance and Z imaginary represent the imaginary impedance

The proton conductivity values of the ZrP/IL material as a function of the mass percentages of IL are presented in Figure 9. It can be clearly seen that the conductivity increases up to a certain IL mass percent then decreases. For example, the ZrP/1-ethyl-3-methylimidazolium ethyl sulfate increases to a maximum of 2.26×10^{-2} S cm $^{-1}$ at a mass percent of 0.8%. This pattern might be attributed to the fact that there is a maximum amount of intercalation of guest molecules into the layered ZrP structure [150]. The layered structure of ZrP is represented in Figure 10. It is anticipated that the ionic liquids might have been intercalated in between the ZrP layers. More discussion on the intercalation will be provided at the end of the chapter. The maximum proton conductivity values are summarized in Table 3.

The enhancement in the proton conductivity can be further investigated by examining the molecular structure of the ionic liquids used in this work as shown in Figure 6. The three ionic liquids [EMIM][ESO_4], [BMIM][DCA], and [BMIM] [OTF] are all hydrophilic. Moreover, it appears that they provided additional sites for proton transfer and hydrogen bonding network [152]. The maximum proton conductivity was observed in the case of [EMIM][ESO_4].

So far, and based on the chemical structure, the conductivity trend might be explained in terms of hydrogen bonding. In the literature, it is confirmed that [EMIM][ESO_4] has the highest ability for hydrogen bonding among the three ionic liquids followed by [BMIM][DCA], and [BMIM] [OTF] [153]. The polarity of

[EMIM][ESO_4] is also the highest with β value of around 0.66 compared to 0.6 for [BMIM][DCA], and 0.49 for [BMIM] [OTF] [154]. Therefore, the hydrogen bonding between the [EMIM][ESO_4] and the P-OH in the ZrP is expected to be the strongest, resulting in stronger bonding and eventually more hopping sites for protons. Furthermore, the structural arrangement of [ESO_4] anion increases the possibility of forming multiple H-Bonding which provides multiple paths for proton hopping. These reasons might explain the highest conductivity value observed in the case of [EMIM][ESO_4] ionic liquid.

[BMIM] [OTF] enhanced the conductivity of the ZrP material. However, when compared to ZrP/[EMIM][ESO_4], the ZrP/[BMIM] [OTF] gave a lower proton conductivity. Although hydrophilic, the [BMIM] [OTF] ionic liquid can act as an inductive electron withdrawal, forming fluoroalkyl structural domains instead of hydrogen bonding [153]. Hence, resulting in a weak hydrogen bonding with the OH from the ZrP. Also, the [OTF] anion repels water molecules and it will act as a barrier between the water molecules, ZrP and the ionic liquid.

The proton conductivity of powder ZrP with ionic liquids was reported in literature in only one study. A layered ZrP material was prepared in a solvent of 1-ethyl-3-methylimidazolium hexafluorophosphate. The proton conductivities were 0.0145 S cm^{-1}(at 363 K, 95% relative humidity) and 1.1×10^{-5} S cm^{-1} at 503 K [139].

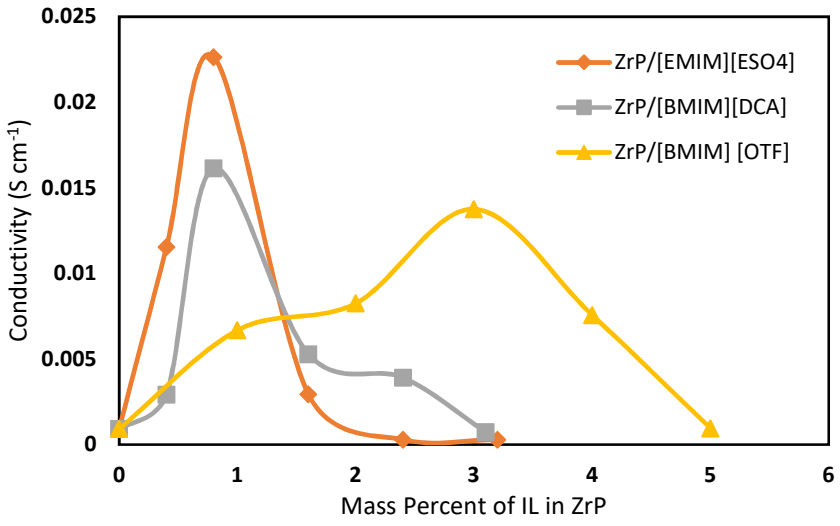

Figure 9. Conductivity versus IL mass percentages for ZrP/IL materials

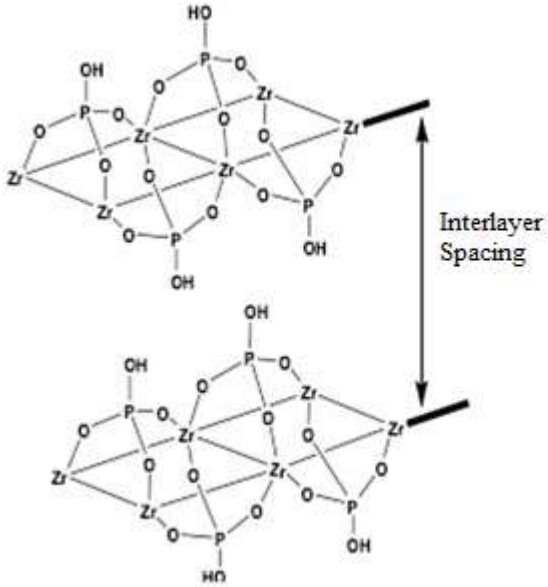

Figure 10. ZrP layered structure [151]

4.3.Thermogravimetric Analysis (TGA)

The water uptake properties and the thermal stability of ZrP/IL materials were investigated in this work by performing thermogravimetric analysis (TGA). The TGA studies were carried out in N_2 atmosphere at a heating rate of 10 ^oC/min. The TGA was performed on the samples that produced the highest conductivity values. The TGA results are shown in Figure 11 and Figure 12.

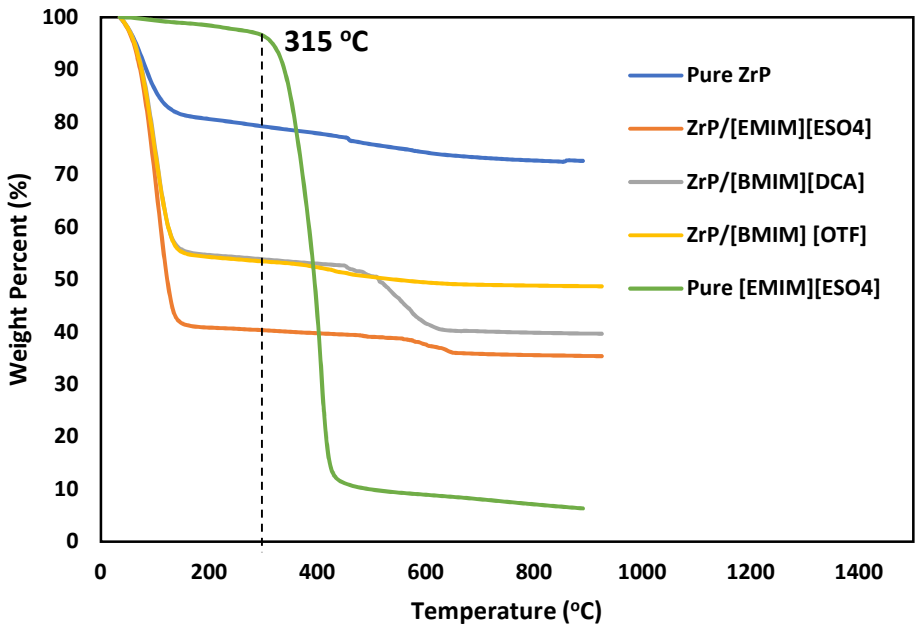

Figure 11. TGA data for ZrP and ZrP/IL samples

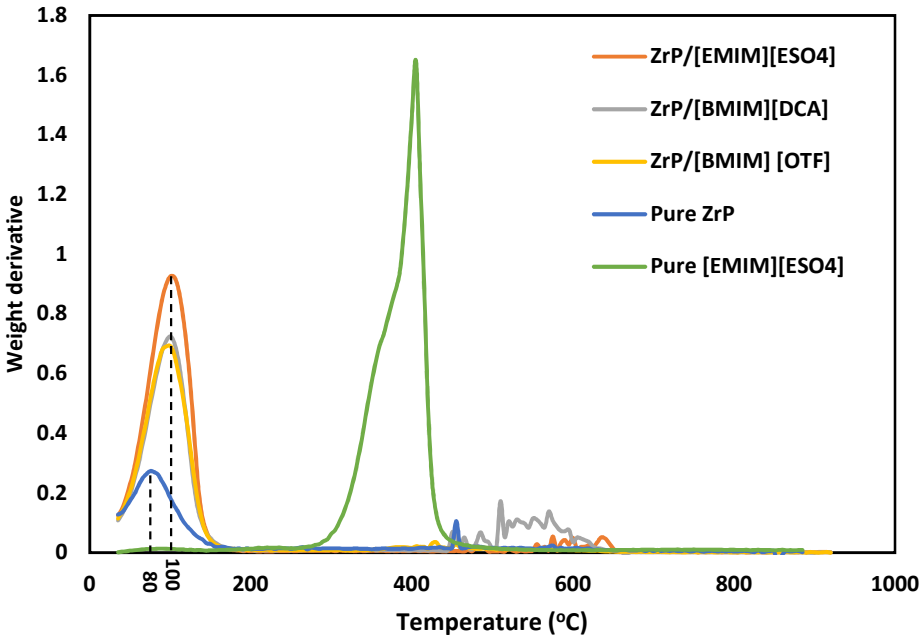

Figure 12. DTG curves for ZrP and ZrP/IL samples

Examining the TGA and DTG curves shows the following observations:

1) Pure ionic liquid ([EMIM][ESO_4]) showed negligible weight loss up to 315 °C.

2) Pure ZrP material showed a weight loss of 20% up to a 120 °C with a maximum loss at 80 °C. This percent is associated with 4 molecules of water in the ZrP structure $Zr(HPO_4)_2.4H_2O$. From literature, the water weight loss occurred mainly at around 100 °C, which is consistent with the results of this study [155].

3) ZrP/[EMIM][ESO_4] showed a major weight loss of 60% up to 150 °C with a maximum weight loss at 100 °C. The same trend is observed in the other two ZrP/IL samples; [BMIM][DCA], and [BMIM] [OTF].

4) The pure and modified samples showed a second stage of weight loss at temperatures above 400 °C. This can be attributed to the condensation of the phosphate groups to form pyrophosphate [155].

It is evident that modifying ZrP with the ionic liquid increased the water content in the samples. To summarize: 1) the water uptake of all ZrP/IL samples is higher than that of the ZrP sample with no ionic liquids, 2) ZrP/[EMIM][ESO_4] sample has the

highest water uptake, followed by ZrP/[BMIM][DCA] and ZrP/[BMIM] [OTF]. These results are consistent with the conductivity results. The ZrP/IL samples had higher conductivity compared to the ZrP sample with no ionic liquids and that ZrP/[EMIM][ESO_4] sample has the highest conductivity value and ZrP/[BMIM] [Otf] has the lowest.

TGA studies in the literature showed that when all the water molecules are removed, zirconium pyrophosphate ZrP_2O_7 is formed at temperatures around 1000 ºC [156]. Assuming that at the final TGA temperature, only ZrP_2O_7 is left and that all the losses are attributed to water losses, the ratio of the water molecules to the molecules of ZrP_2O_7 can be calculated at each temperature as shown in Figure 13. It is evident that the number of water molecules loss for the modified samples has drastically increased compared to the pure ZrP material. It is also shown that the ZrP/[EMIM][ESO_4] has the highest number of water molecules, with moles H_2O/moles ZrP_2O_7 value of around 26. This agrees with the fact that it has the highest water uptake and highest conductivity.

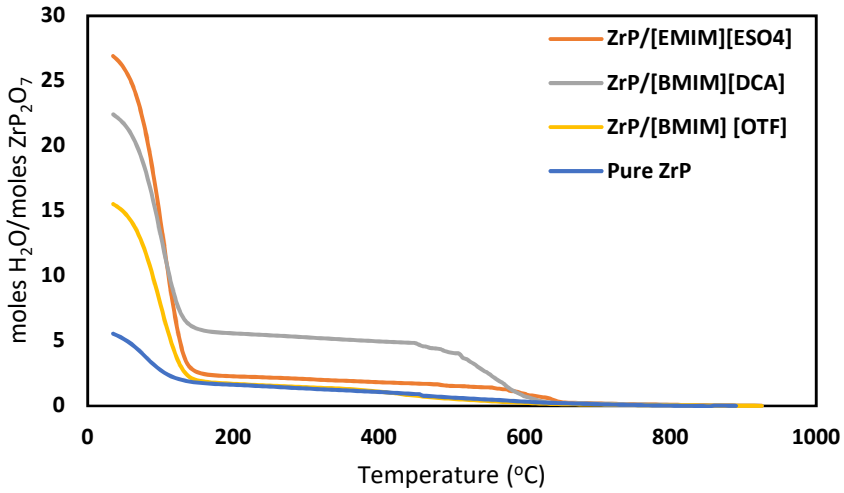

Figure 13. Ratio of water molecules lost to molecules of zirconium pyrophosphate for pure ZrP and ZrP/IL modified samples

4.4. Fourier Transform Infrared Spectroscopy (FTIR)

FTIR analysis was performed to investigate the chemistry and chemical interactions in the modified ZrP/IL material. FTIR analysis was performed on pure ZrP sample and on the samples with highest conductivity values. The FTIR spectra for the ZrP/IL samples are shown in Figure 14. All the samples showed a shoulder at around 960-980 cm^{-1}. This shoulder is characteristics for the P-OH stretching [157]. The

samples also showed peaks and shoulders at around 1100 cm^{-1} and 1220 cm^{-1}. These are attributed to the antisymmetric vibrational stretch in the peaks of the PO_4 groups [139]. At 1630 cm^{-1}, sharp peaks were observed. These peaks are characteristic of molecular water trapped in the lattice structure [158]. All the samples appeared to contain a certain amount of lattice water (water molecules held in the crystal structure by hydrogen bond). O-H stretching also occurred at around 2400 cm^{-1} in all the samples. The ZrP/IL samples exhibited absorption bands at around 2930 cm^{-1} due to the vibration of the symmetrical C-H alkyl groups [159]. The peaks at 3460 cm^{-1} are a result of water molecules vibrations [160].

In general, the spectra for pure ZrP and the modified ZrP/IL were similar. However, the intensity of the O-H peaks at 1630 cm^{-1} and at 3460 cm^{-1} was higher for all the modified ZrP/IL material compared to the pure ZrP sample. The increase in intensity might be an indication of more water in the modified samples [158]. This is in agreement with the TGA results that showed higher water uptake in the modified samples. Presumably, more water is contained in the lattice structure due to the modification with the IL component. Another difference between the pure ZrP material and the modified ZrP/IL materials is the bands at 1100 cm^{-1} and 1630 cm^{-1}. It can be observed that these bands had shifted a little bit to the left for the modified materials compared to the pure ZrP sample. This shift can be a sign of the ionic liquids intercalation within the ZrP layers.

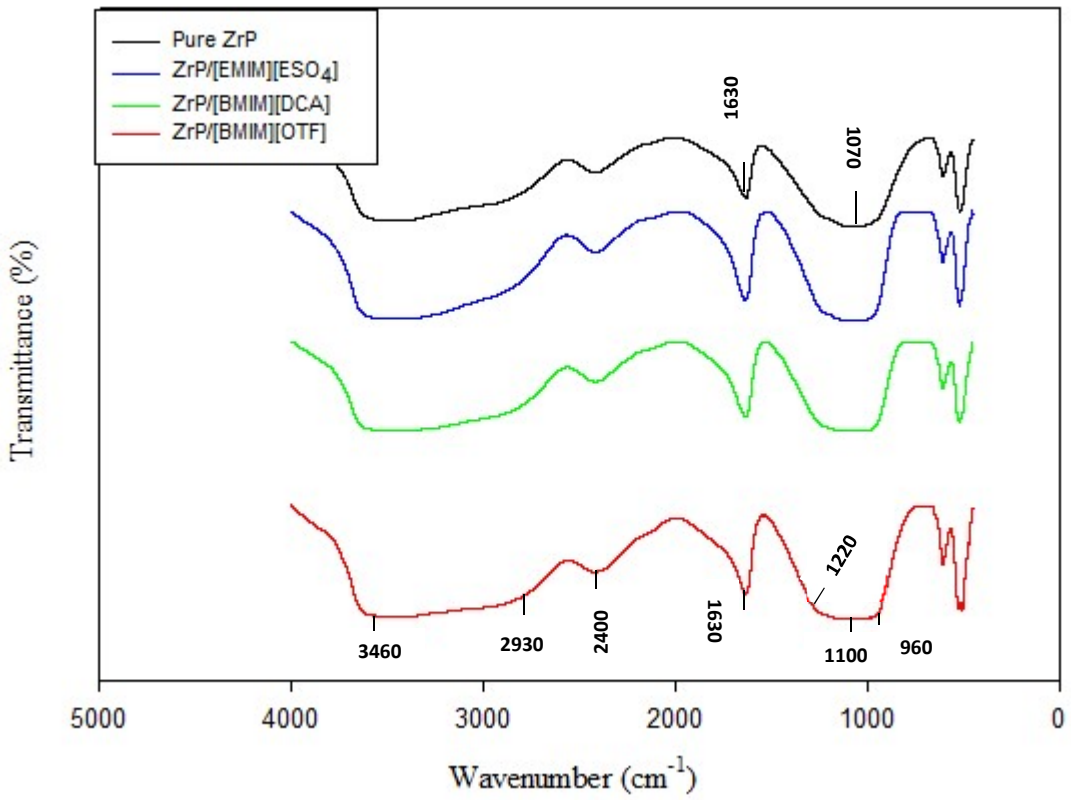

Figure 14. FTIR spectra for ZrP and ZrP/IL modified materials

4.5. X-Ray diffraction (XRD)

XRD was performed for the pure ZrP material prepared in this work to investigate the crystal structure of the prepared samples. The XRD pattern is shown in Figure 15. In general, the samples appear to be amorphous as broad peaks have appeared, but they also possess some crystal structure. The amorphous nature of the ZrP material allows the localization of water molecules in between the its layers [161]. As the crystallinity of the material increases, the amount of surface water decreases significantly [161].

From Figure 15, it can be seen that intense peaks appeared at different 2θ values, where θ is the angle at which the incident beam is deflected. XRD can be successfully employed to calculate the changes in the d-spacing for materials through Bragg's law [162]. For the pure ZrP material, reflections had appeared at 2θ of around 20.4°, 34.3°, 42° and 53.4°. These reflections were compared to literature pure ZrP reflections and the results were in agreement with the results from this study [155]. For the ZrP/[EMIM][ESO_4], reflections appeared at 23.7°, 34.3°, 43° and 53.1°.

ZrP/[BMIM][DCA] showed reflections at 19.16°, 34.1°, 43.7° and 54°. The ZrP/[BMIM] [Otf] exhibited reflections at 2θ of 19.1°, 34° and 52.8°.

From the values of 2θ and using Bragg's law in equation 4.1, the d-spacing can be calculated.

$$\lambda = 2\,d\sin(\theta) \qquad (4.1)$$

The values of d-spacing are shown in Table 4.

Table 4. d-spacing for the pure ZrP and the modified ZrP/IL samples

Sample	d-Spacing (A°)
ZrP (No IL)	4.23
ZrP//[EMIM][ESO_4]	3.26
ZrP/[BMIM][DCA]	4.5
ZrP//[BMIM][OTF]	4.52

ZrP/[BMIM][DCA] and ZrP/[BMIM][OTF] has shown a change in the lattice structure with 4.5 A° and 4.52 A°. This change might be attributed to intercalation. When the ionic liquids are intercalated within the layers of ZrP, the distance between the layers is expected to change. However, ZrP/[EMIM][ESO_4] the value of d-spacing decreased. One possible explanation would be the formation of multiple H-bonding on the surface of the ZrP resulting in a change in the d-spacing [163].

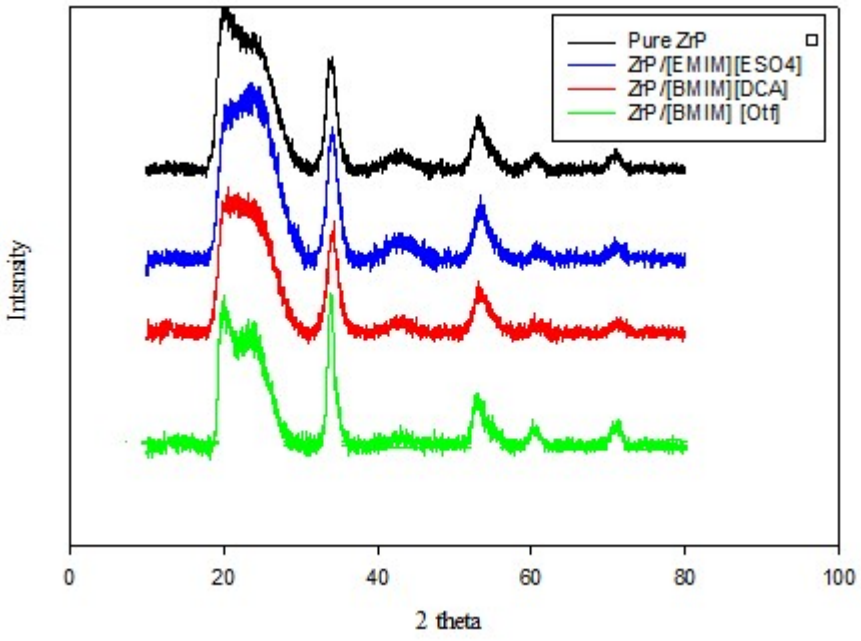

Figure 15. XRD pattern for pure ZrP and ZrP/IL modified samples

4.6. Raman Spectroscopy

Raman Spectroscopy was performed on the pure ZrP material and the three best conducting modified ZrP/IL materials to identify the differences in the main functional groups between the pure material and the modified ones. The Raman spectra are presented in Figure 16. As shown in Figure 16, all the samples showed a band at around 280 cm^{-1}. This band represent Zr-O interaction from the ZrP [164]. At around 1050 cm^{-1}, a band had appeared in all the samples. This band represent the P-O stretching mode [164].

The pure ZrP material showed bands at around 1200 cm^{-1} and 1400 cm^{-1}. However, these bands disappeared from the modified ZrP/IL materials. These bands are associated with the vibrations of P-OH stretching region [165]. This disappearance, is a sign of intercalation where the guest ionic liquid molecules are contained within the interlayer space of the host ZrP. The interaction occurs between the anions of the ionic liquids and the P-OH from the ZrP. These results agree with the FTIR results, that showed an increase in the intensity of the O-H bond in the modified ZrP/IL samples, and the XRD results that showed a change in the d-spacing in the modified materials.

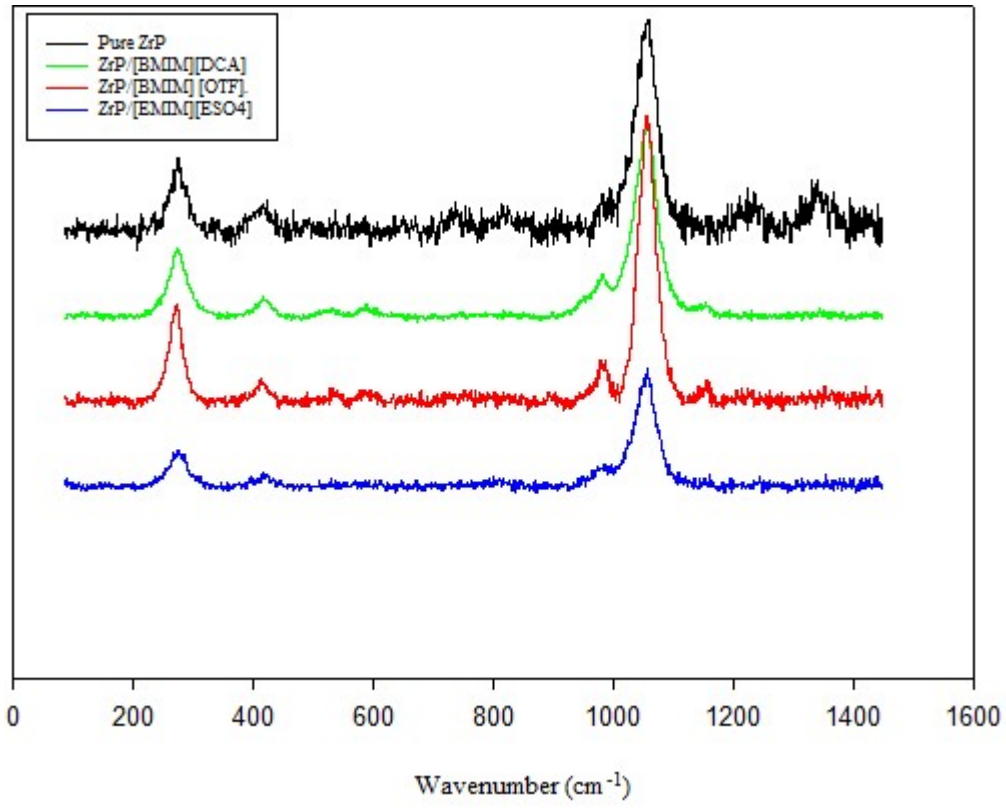

Figure 16. Raman Spectra of pure ZrP and modified ZrP/IL materials.

4.7. Scanning Electron Microscopy (SEM)

The scanning electron microscopy (SEM) images are shown in Figure 17 and Figure 18. Figure 17 shows a top view for the morphology of pure ZrP material. The particles show some hexagonal, plate-like shape. It also shows piles of smaller plate-like particles (less than 1 μm) deposited. Figure 18 shows the morphology of the modified ZrP/IL material. The samples are: ZrP/[EMIM][ESO_4], ZrP/[BMIM][DCA] and ZrP/[BMIM] [OTF]. In general, a change of morphology is observed. In the case of ZrP/[EMIM][ESO_4] for example (Figure 18 c and d), smaller plate like particles were formed. The same observation can be made on for the ZrP/[BMIM][DCA] and ZrP/[BMIM] [OTF] (Figure 18 e-h). It appears that adding the ionic liquid component decreased the particles sizes and changed the crystals shapes in general.

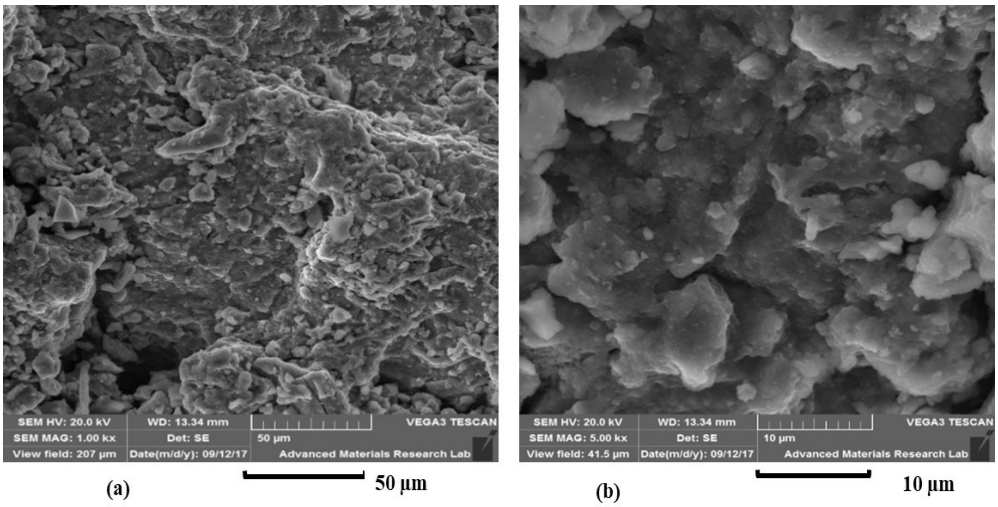

Figure 17. Scanning Electron Microscopy (SEM) image for pure ZrP at different magnifications. (a) at 1000X and (b) at 5000X

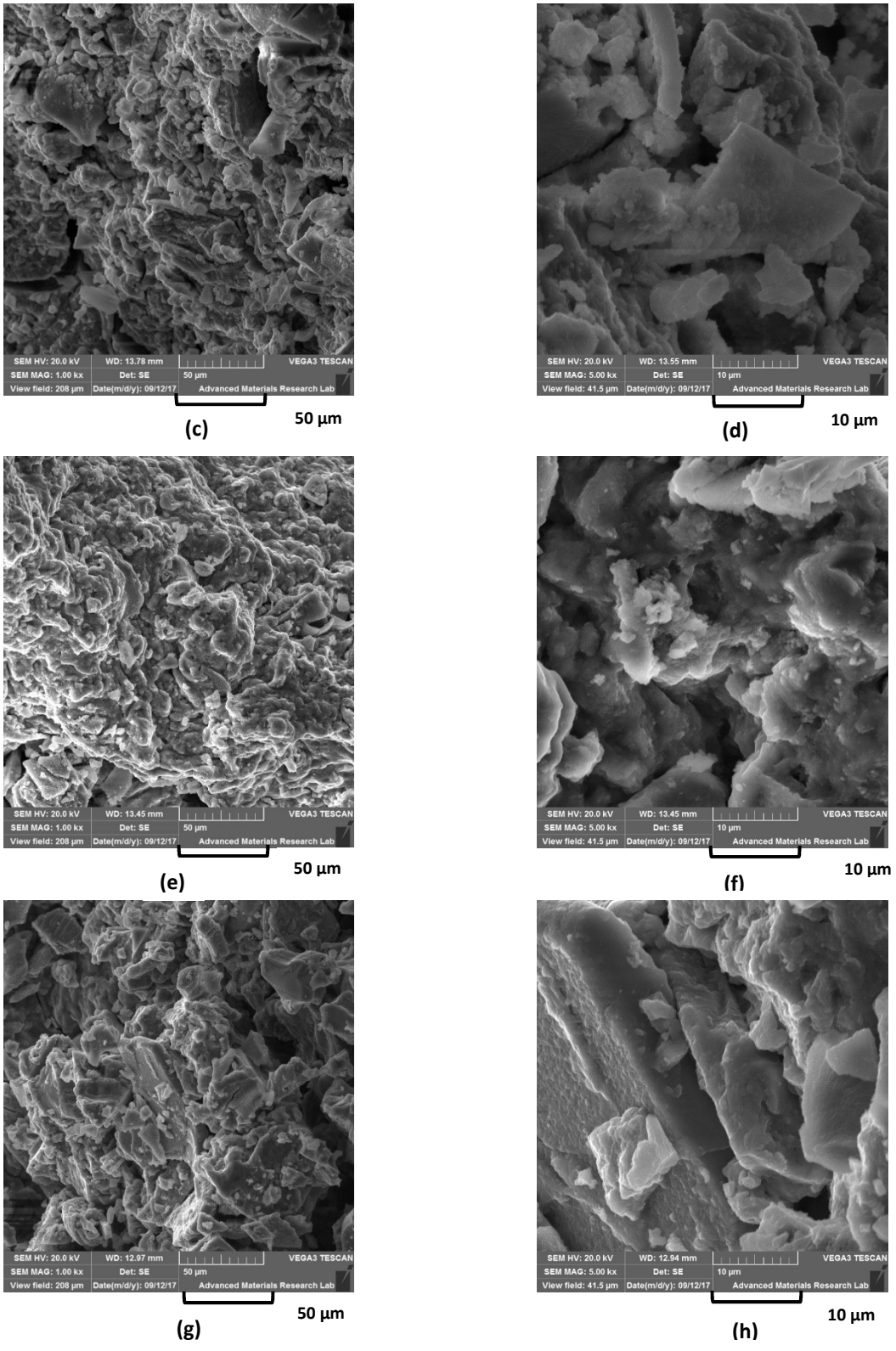

Figure 18. Scanning Electron Microscopy (SEM) images for ZrP/IL samples. (c) and (d) ZrP/[EMIM][ESO_4], (e) and (f) ZrP/[BMIM][DCA], and (g) and (h) ZrP/[BMIM][OTF] at 1000X and 5000X

4.8. Conductivity at High Temperature

The proton conductivity at higher temperatures was investigated in this work. The ZrP/IL materials were heated in a tube furnace at 200ºC and anhydrous conditions, under vacuum. The proton conductivity was evaluated using EIS. The results are summarized in Table 5.

Table 5. Conductivity of ZrP/IL samples after heating at 200 ºC and anhydrous conditions

Sample	Conductivity (S cm^{-1})
ZrP/[EMIM][ESO_4]	3.72×10^{-4}
ZrP/[BMIM][DCA]	4.36×10^{-4}
ZrP/[BMIM] [OTF]	4.75×10^{-4}

As indicated in the table, the conductivity results show a decrease of about two orders of magnitude. The decrease in conductivity is attributed to the loss of water content due to evaporation. Although the conductivity of the ZrP/IL materials has decreased upon heating to 200ºC, but the results are still promising, and the performance is still better than the performance of Nafion. The behavior of Nafion at low humidified conditions was studied in literature. The conductivity of Nafion is 1.40×10^{-4} S cm^{-1} at 30ºC and a relative humidity of 34% [166]. The reported conductivity in this work is in the order of 10^{-4} S cm^{-1} at 200 °C, at completely anhydrous conditions. This conductivity considered a high anhydrous proton conductivity [167].

4.9. Discussion

Overall, it can be seen that the ionic liquids have enhanced the conductivity of the ZrP materials. The increase in the conductivity might be attributed to several reasons. Raman spectroscopy analysis confirmed the intercalation of ionic liquids into ZrP layers. It appears that the ionic liquids have also formed hydrogen bonding with the O-H from the ZrP molecules. This intercalation and hydrogen bonding have changed the morphology of the particles (as seen in SEM, XRD), and increased the water uptake (as seen in TGA analysis). Hence, provided additional pathways for the

proton transfer and effective proton hopping sites. The proposed interaction mechanism is represented in Figure 19 with taking [EMIM][ESO_4] as an example.

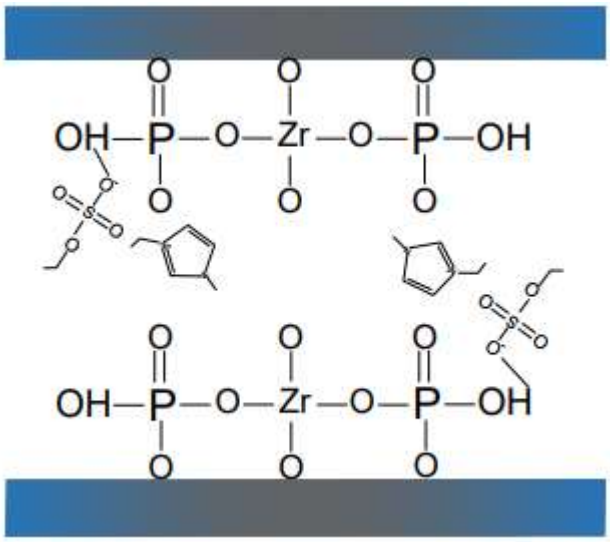

Figure 19. Proposed intercalation mechanism for ILs in between the ZrP layers

In addition, from the XRD results, the ZrP in this study was found to be mostly amorphous. This amorphous structure allows the localization of water molecules in between its layers [161]. It was also found that as the crystallinity of the material decreases, the surface water increases [161]. Moreover, all the ionic liquids chosen in this experiment are hydrophilic which is expected to increase the water content inside the ZrP powder samples and in return increase the conductivity of the samples. The latter suggests that the transfer of protons in ZrP material is highly dependent on water. Therefore, the amorphous nature of the ZrP along with the hydrophilicity of the ionic liquids and the hydrogen bonding that is formed between the ionic liquids and ZrP might explain the increase in conductivity of the modified materials.

The ZrP in this study is presented as zirconium mono-hydrogen phosphate. The formation of zirconium dihydrogen phosphate is unfavorable under the conditions of this study [163]. If zirconium dihydrogen phosphate was formed, it is expected that the ZrP would have bounded to water molecules up to a higher temperature [163]. Since the water molecules in ZrP were readily removed from the structure, as was shown from the TGA curves, it can be assumed that they were held by the hydrogen bonds and not coordinated to the zirconium atom [163]

Chapter 5. Results and Discussion – Glycerol

5.1. Introduction

A sub-objective of this study, was to investigate the effect of the incorporation of glycerol (GLY) on the conductivity of the ZrP material. Glycerol has been shown previously to enhance proton conductivity of ZrP. Therefore, it was investigated in this project for a possible future combination with ionic liquid to produce a PEM fuel cell membrane based on ZrP/IL/GLY.

Glycerol was added to the $ZrOCl_2$ solution in mass percentages ranging between 2% and 4% followed by the precipitation reaction with H_3PO_4 to prepare the ZrP/GLY modified materials. After the preparation, the best conducting sample was subjected to characterization with EIS, TGA and FTIR. Some of the physical characteristics of glycerol are summarized in. The chemical structure of glycerol is shown in Figure 20.

Table 6. Physical properties of glycerol at 20 ºC [168]

Property	Value
Density	1.261 g/m^3
Viscosity	1.5 Pa.S
Boiling point	290 ºC
Hydrophilic/hydrophobic	Hydrophilic
Surface tension	64 × 10^{-3} N/m

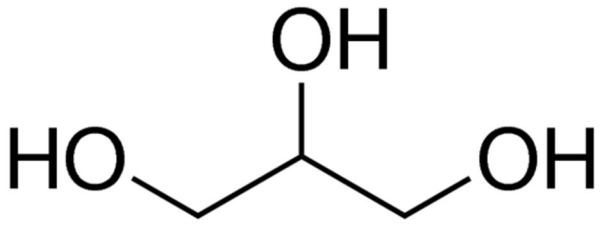

Figure 20. Chemical structure of glycerol

5.2. Conductivity measurements

Electrochemical impedance spectroscopy (EIS) analyses (Nyquist Plots) were performed on the ZrP/GLY materials. The EIS spectra of the best conducting glycerol sample is shown in Figure 21. The electrolyte resistance of the ZrP/GLY materials was found from the extrapolation of the EIS spectra at the high frequency range to find their intercept with the x-axis. Equation 3.2 was then applied to calculate the conductivity. The conductivity of the best ZrP/GLY material was obtained with 3% by mass GLY and the value was found to be 1.80×10^{-2} S cm^{-1}.

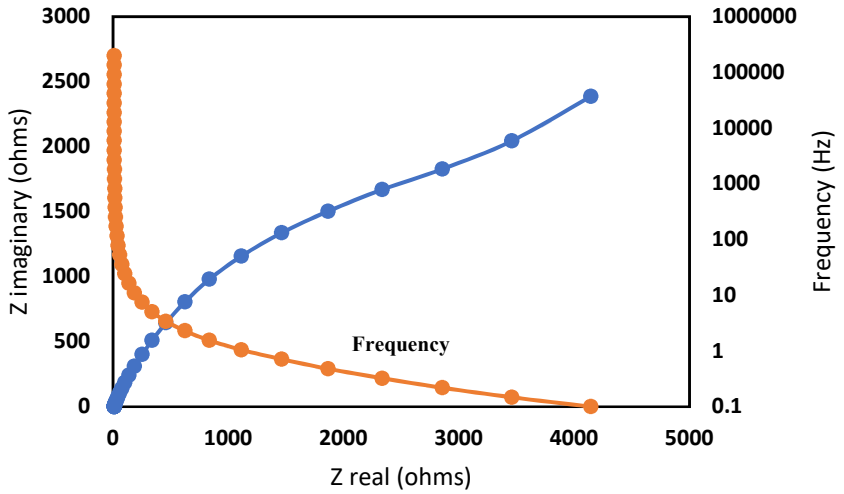

Figure 21. Nyquist plot for the best conducting ZrP/GLY sample (3% by mass GLY). Z real represents the real impedance and Z imaginary represent the imaginary impedance

The proton conductivity of the ZrP/GLY material as a function of the mass percentage of GLY is presented in Figure 22.

As shown in Figure 22, the ZrP/GLY materials follow a similar trend as the ZrP/IL materials discussed earlier. The conductivity increases and reached a maximum value of 1.80×10^{-2} S cm^{-1} at 3% by mass GLY. After that, the conductivity starts to decrease. The glycerol is also anticipated to have been intercalated in between the ZrP layers and hence, there will be a certain amount of GLY molecules that can be admitted in between the layers.

The addition of glycerol to the ZrP material has clearly enhanced its proton conductivity. The increase in conductivity can be explained from the chemical structure of glycerol. As seen in Figure 20, glycerol has three O-H groups and therefore, its

presence within the ZrP material will increase the overall number of the O-H groups inside the modified material. This is expected to provide more proton transport sites for hopping. Hence, the proton conductivity will be enhanced.

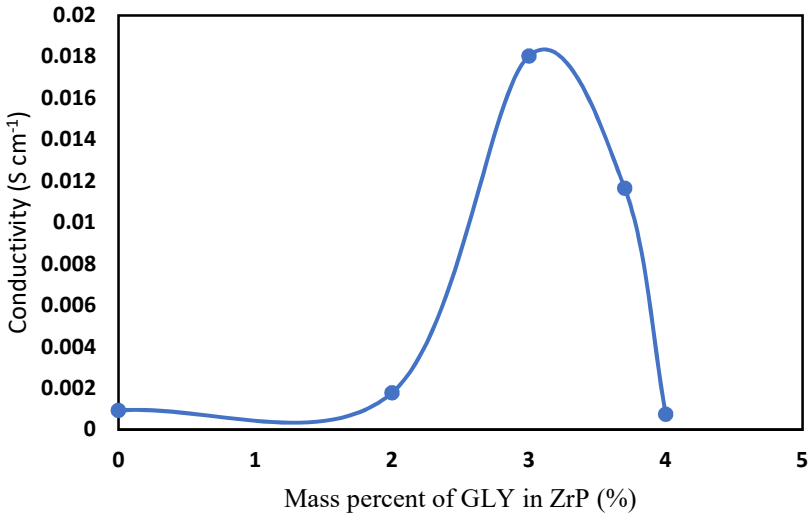

Figure 22. Conductivity versus GLY mass percentages for ZrP/GLY materials

5.3.Thermogravimetric Analysis (TGA)

The thermal stability of the best conducting ZrP/GLY material, along with its water uptake were studied using TGA. The results of the TGA are shown in Figure 23 and Figure 24.

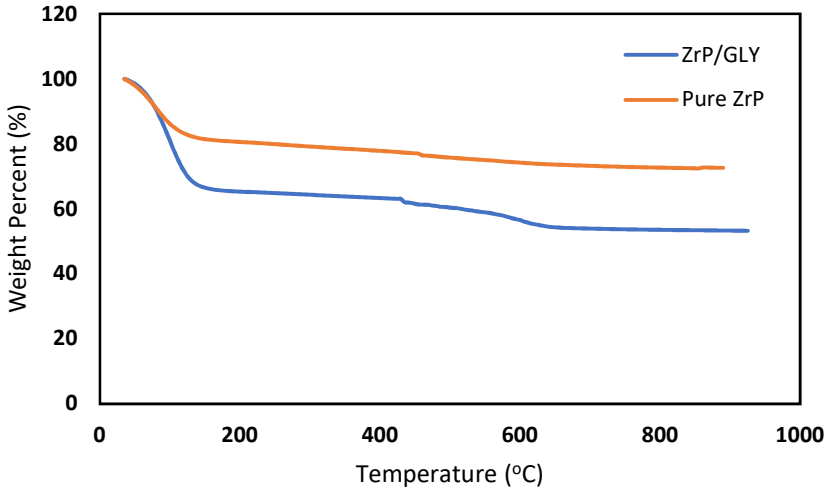

Figure 23. TGA curves for pure ZrP and ZrP/GLY samples

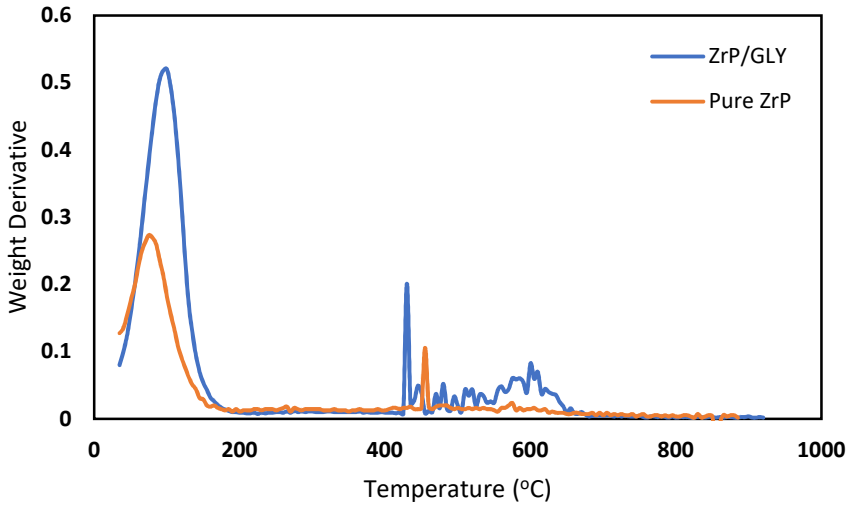

Figure 24. DTG curves for pure ZrP and ZrP/GLY samples

The TGA analysis of the ZrP/GLY material showed a weight loss of about 30% at temperatures less than 200 °C with a maximum loss at 105 °C. The losses after 400 °C are attributed to to the condensation of the phosphate group in the ZrP material between the P-OH groups [22].

The incorporation of glycerol within the ZrP material has enhanced the water content of the samples. This is evident from Figure 24 that shows a higher water uptake of the modified ZrP/GLY sample compared to the pure ZrP sample. These results are consistent with the conductivity results in which the modified ZrP/GLY material had higher conductivity compared to the pure ZrP material.

5.4. Fourier Transform Infrared Spectroscopy (FTIR)

The FTIR spectra of the modified ZrP/GLY material is shown in Figure 25. The main peaks for the modified ZrP/GLY are the same as in section 4.4. P-OH stretching bands appeared at around 1000 cm^{-1}. The vibrational band of the PO_4 group appeared at around 1200 cm^{-1}. The molecular water and O-H stretching vibrations appeared at 1634 cm^{-1} and 2400 cm^{-1}. C-H alkyl group shoulder appeared at 2920 cm^{-1}.

Similar to the ZrP/IL material, the ZrP/GLY material showed an increase in intensity for the O-H peaks at 1630 cm^{-1} and at 3460 cm^{-1}. This is because the glycerol has increased the number of OH molecules in the ZrP material.

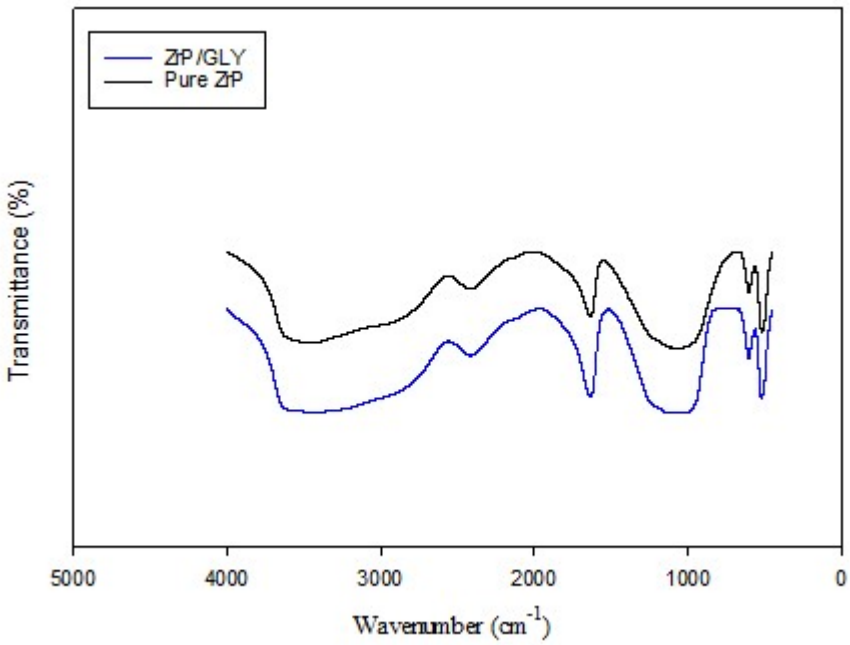

Figure 25. FTIR spectra for pure ZrP and ZrP/GLY modified material

Chapter 6. Conclusions and Recommendations

6.1. Conclusions

In this study, a proton conducting material for PEM fuel cells was synthesized based on ionic liquids and ZrP. Seven ionic liquids were tested: [EMIM][ESO_4], [BMIM][DCA], [BMIM] [OTF], [EMIM][AC], [BMIM] [TFA], [DEMA][OMS], [DEMA][OTF]. Among all the ionic liquids tested, [EMIM][ESO_4], [BMIM][DCA], [BMIM] [OTF] produced the highest proton conductivities. The modified materials in this project were prepared by the addition of the ionic liquids to a solution of $ZrOCl_2$, followed by a precipitation reaction with H_3PO_4 to prepare the ZrP/IL materials.

The conductivities of the best conducting samples were 2.26×10^{-2}, 1.36×10^{-2} and 1.61×10^{-2} S cm^{-1}, achieved with the ionic liquids [EMIM][ESO_4], [BMIM][DCA], [BMIM] [OTF] respectively. The conductivity of the pure ZrP material that was produced in this work was 9.24×10^{-4} S cm^{-1}.

Overall, this work showed that the incorporation of ionic liquids within the ZrP material enhances the conductivity of the ZrP material by orders of magnitude. The increase in conductivity is attributed to the following reasons: 1) the intercalation of the ionic liquids in between the layers of the ZrP which provided additional hopping sites, 2) the hydrogen bonding that was formed between the anions of the ionic liquids and the P-OH from the ZrP, 3) the hydrophilicity of all the ionic liquids in this study, which have increased the water content of the ZrP material and 4) the amorphous nature of the ZrP that helps in trapping surface water and hence increasing the water content of the material. These conclusions were supported by the results of TGA, SEM, XRD, FTIR and Raman spectroscopy.

The performance of the ZrP/IL materials at high temperature was investigated at temperature of 200 ^oC and anhydrous conditions. Although the conductivity decreased, the results were better than that for Nafion membrane, which loses hydration and shows a drastic decrease in conductivity when operated above 100 ^oC. Moreover, a conductivity in the range of 10^{-4} at 200 ^oC is considered a high anhydrous proton conductivity [167].

The proton conducting and water uptake characteristics of the incorporation of glycerol within the ZrP material was also studied in this project. It was proved that

glycerol has enhanced the water content of the ZrP samples by increasing the number of O-H groups in the material which increases the proton hopping sites. Therefore, it is anticipated that incorporating a combination of glycerol and ionic liquids within ZrP material would be a promising electrolyte material for high temperature PEM fuel cells and is worth future investigation.

6.2. Recommendations for Future Work

1) Prepare composite membranes based on the ionic liquids that produced highest conductivity, and study their performance at high temperatures.
2) Prepare composite membrane based on the combination between ionic liquids and glycerol and investigate their proton conducting characteristics, water uptake and their performance at high temperatures.
3) Study protic ionic liquids with similar anions to the ones tested in this study, in order to get a more understanding on the type of ionic liquids that will maximize the proton conductivity of the ZrP material.
4) Prepare zirconium phosphate in methods other than the precipitation method and study the effect on the conductivity and thermal stability.
5) Investigate the effect of zirconium phosphate pH on the conductivity of the ZrP material and the size of the particles.
6) Prepare water isotherm to examine the effect of water content on the conductivity of the ZrP.
7) Perform particle size distribution analysis for the pure ZrP and the modified samples.
8) Synthesize proton conducting material based on PBI, ZrP and ionic liquids and study the proton conductivity and high temperature behavior.

References

[1] M. Jacobson, "Review of solutions to global warming, air pollution, and energy security," *Energy & Environmental Science,* vol. 2, pp. 148–173, 2009.

[2] S. McPhail, V. Cigolotti and A. Moreno, *Fuel Cells in the Waste-to-Energy Chain: Distributed Generation Through Non-Conventional Fuels and Fuel Cells*, London: Springer-Verlag London, 2012.

[3] O. Yarguddi and A. Dharme, "Fuel Cell Technology: A Review," *International Journal of Innovative Research in Science, Engineering and Technology,* vol. 3, no. 7, pp. 14668-14673, 2014.

[4] E. Kjeang, *Microfluidic Fuel Cells and Batteries*, Springer International Publishing, 2014.

[5] C. Rayment and S. Sherwin, "Introduction to Fuel Cell Technology," University of Notre Dame, Notre Dame, 2003.

[6] G. Scherer, *Advances in Polymer Science*, Springer, 2008.

[7] G. Acres, "Recent advances in fuel cell technology and its applications," *Journal of Power Sources,* vol. 100, no. 1-2, pp. 60-66, 2001.

[8] "A Historical Perspective of Fuel Cell Technology in the 20th Century," *Journal of The Electrochemical Society,* vol. 149, no. 7, pp. S59-S67, 2002.

[9] J. Andújar and F. Segura, "Fuel cells: History and updating. A walk along two centuries," *Renewable and Sustainable Energy Reviews,* vol. 13, no. 9, p. 2309–2322, 2009.

[10] U. Lucia, "Overview on fuel cells," *Renewable and Sustainable Energy Reviews,* vol. 30, p. 164–169, 2014.

[11] F. Barbir, *Sustainable World : PEM Fuel Cells : Theory and Practice (1)*, Academic Press, 2005.

[12] F. Barbir, *PEM Fuel Cells : Theory and Practice (2)*, Academic Press, 2012.

[13] J. Zhang, *PEM Fuel Cell Electrocatalysts and Catalyst Layers: Fundamentals and Applications*, Springer Science & Business Media, 2008.

[14] M. Ternan, "The potential of direct hydrocarbon fuel cells for improving energy efficiency," in *EIC Climate Change Technology*, Ottawa, 2006.

[15] J. Zaidi, "Research Trends in Polymer Electrolyte Membranes for PEMFC," in *Polymer Membranes for Fuel Cells*, Springer US, 2009, pp. 7-25.

[16] H. Khakdaman, "A Two Dimensional Model of a Direct Propane Fuel Cell with an Interdigitated Flow Field," Ph.D. dissertation, University of Ottawa, Ottawa, 2012.

[17] J. Zhang, Z. Xie, J. Zhang, Y. Tang, C. Song, T. Navessin, Z. Shi, D. Song, H. Wang, D. Wilkinson, Z.-S. Liu and S. Holdcroft, "High temperature PEM fuel cells," *Journal of Power Sources,* vol. 160, p. 872–891, 2006.

[18] V. McConnell, "High-temperature PEM fuel cells: Hotter, simpler, cheaper," *Fuel Cells Bulletin,* vol. 2009, pp. 12-16, 2009.

[19] L. Niedrach, "The Performance of Hydrocarbons in Ion Exchange Membrane Fuel Cells," *Journal of The Electrochemical Society,* vol. 109, pp. 1092-1096, 1962.

[20] Q. Li, R. He, J. O. Jensen and N. Bjerrum, "Approaches and Recent Development of Polymer Electrolyte Membranes for Fuel Cells Operating above 100 °C," *Chemistry of Materials,* vol. 15, pp. 4896-4915, 2003.

[21] A. Al-Othman, A. Y. Tremblay, W. Pell, S. Letaief, T. Burchell, B. Peppley and M. Ternan, "Zirconium phosphate as the proton conducting material in direct hydrocarbon," *Journal of Power Sources,* vol. 195, p. 2520–2525, 2010.

[22] A. Al-Othman, A. Tremblay, W. Pell, S. Letaief, Y. Liu, B. Peppley and M. Ternan, "A modified silicic acid (Si) and sulphuric acid (S)eZrP/PTFE/glycerol composite membrane for high temperature direct hydrocarbon fuel cells," *Journal of Power Sources,* vol. 224, pp. 158-167, 2013.

[23] H. Zhang and P. K. Shen, "Recent Development of Polymer Electrolyte Membranes for Fuel Cells," *Chemical Reviews,* vol. 112, no. 5, p. 2780–2832, 2012.

[24] B. Qiu, B. Lin and F. Yan, "Ionic liquid/poly(ionic liquid)-based electrolytes for energy devices," *Polymer International,* vol. 62, no. 3, pp. 335-337, 2013.

[25] S. Haile, "Fuel cell materials and components," *Acta Materialia,* vol. 51, no. 19, p. 5981–6000, 2003.

[26] S. Peighambardoust, S. Rowshanzamir and M. Amjadi, "Review of the proton exchange membranes for fuel cell applications," *International journal of hydrogen energy,* vol. 35, no. 17, pp. 9349-9384, 2010.

[27] H. Khakdaman, Y. Bourgault and M. Ternan, "Direct Propane Fuel Cell Anode with Interdigitated Flow Fields: Two-Dimensional Model," *Industrial & Engineering Chemistry Research (ACS Publications),* vol. 49, no. 3, p. 1079–1085, 2010.

[28] M. Alhassan and M. Umar Garba, "Design of an Alkaline Fuel Cell," *Leonardo Electronic Journal of Practices and Technologies,* vol. 5, no. 9, pp. 99-106, 2006.

[29] G. Merle, M. Wessling and K. Nijmeijer, "Anion exchange membranes for alkaline fuel cells: A review," *Journal of Membrane Science,* vol. 377, no. 1-2, pp. 1-35, 2011.

[30] F. Bidault, D. Brett, P. Middleton and N. Brandon, "Review of gas diffusion cathodes for alkaline fuel cells," *Journal of Power Sources,* vol. 187, no. 1, p. 39–48, 2009.

[31] D. Zugic, I. Perovic, V. Nikolic, S. Maslovara and M. Marceta Kaninski, "Enhanced Performance of the Solid Alkaline Fuel Cell Using PVA-KOH Membrane," *International Journal of Electrochemical Science,* vol. 8, no. 1, pp. 949 - 957, 2013.

[32] N. Wagner, M. Schulze and E. Gülzow, "Long term investigations of silver cathodes for alkaline fuel cells," *Journal of Power Sources,* vol. 127, no. 1-2, p. 264–272, 2004.

[33] E. Gülzow and M. Schulze, "Long-term operation of AFC electrodes with CO2 containing gases," *Journal of Power Sources,* vol. 127, no. 1-2, p. 243–251, 2004.

[34] Z. Ma, R. Venkataraman and M. Farooque, "Fuel Cells - Molten Carbonate Fuel Cells: Modeling," in *Encyclopedia of Electrochemical Power Sources*, Amsterdam, Newnes, 2013, pp. 519-532.

[35] E. Antolini, "The stability of molten carbonate fuel cell electrodes: A review of recent improvements," *Applied Energy,* vol. 88, no. 12, p. 4274–4293, 2011.

[36] M. Kawase, "Manufacturing method for tubular molten carbonate fuel cells and basic cell performance," *Journal of Power Sources,* vol. 285, pp. 260-265, 2015.

[37] H. V. P. Nguyen, S. A. Song, D. Seo, J. Han, S. P. Yoon, H. C. Ham, S. W. Nam, R. M. Othman and J. Kim, "Hydrogen sulfide-resilient anodes for molten carbonate fuel cells," *Journal of Power Sources,* vol. 230, pp. 282-289, 2013.

[38] I. Rexed, M. d. Pietra, S. McPhail, G. Lindbergh and C. Lagergren, "Molten carbonate fuel cells for CO2separation and segregation byretrofitting existing plants – An analysis of feasible operatingwindows and first experimental findings," *International Journal of Greenhouse Gas Control,* vol. 35, p. 120–130, 2015.

[39] E. Arato, E. Audasso, L. Barelli, B. Bosio and G. Discepoli, "Kinetic modelling of molten carbonate fuel cells: Effects of cathode water and electrode materials," *Journal of Power Sources,* vol. 330, pp. 18-27, 2016.

[40] J. Milewski, K. Futyma and A. Szczęśniak, "Molten carbonate fuel cell operation under high concentrations of SO2 on the cathode side," *International Journal of Hydrogen Energy,* vol. 41, pp. 1-9, 2016.

[41] T. Leo, "Molten Carbonate Fuel Cells: Theory and Application," in *Comprehensive Renewable Energy*, Danbury, Elsevier, 2012, pp. 247-259.

[42] M. Perry and T. Fuller, "A Historical Perspective of Fuel Cell Technology in the 20th Century," *Journal of The Electrochemical Society,* vol. 149, no. 7, pp. 59-67, 2002.

[43] X. Chen, Y. Wang, L. Cai and Y. Zhou, "Maximum power output and load matching of a phosphoric acid fuel cell-thermoelectric generator hybrid system," *Journal of Power Sources,* vol. 294, pp. 430-436, 2015.

[44] T. Kuwabara, "Fuel Cells - Phosphoric Acid Fuel Cells: Cathodes," in *Encyclopedia of Electrochemical Power Sources*, Newnes, Elsevier, 2009, pp. 557-563.

[45] X. Chen, Y. Wang, Y. Zhao and Y. Zhou, "A Study of Double Functions and Load Matching of a Phosphoric Acid Fuel Cell/Heat-Driven Refrigerator Hybrid System," *Energy,* vol. 101, pp. 359-365, 2016.

[46] N. Sammes, R. Bove and K. Stahl, "Phosphoric acid fuel cells: Fundamentals and applications," *Current Opinion in Solid State and Materials Science,* vol. 8, p. 372–378, 2004.

[47] T. Murahashi, "Fuel Cells - Phosphoric Acid Fuel Cells: Electrolytes," in *Encyclopedia of Electrochemical Power Sources*, Newnes, Elsevier, 2009, pp. 564-567.

[48] P. Yang, H. Zhang and Z. Hu, "Parametric study of a hybrid system integrating a phosphoric acid fuel cell with an absorption refrigerator for cooling purposes," *International Journal of Hydrogen Energy,* vol. 41, pp. 3579-3590, 2016.

[49] L. Blomen and M. Mugerwa, *Fuel Cell Systems*, Springer Science & Business Media, 2013.

[50] N. Minh, "Solid oxide fuel cell technology—features and applications," *Solid State Ionics,* vol. 174, p. 271–277, 2004.

[51] S. Singhal, "Advances in solid oxide fuel cell technology," *Solid State Ionics,* vol. 135, p. 305–313, 2000.

[52] O. Yamamoto, "Solid oxide fuel cells: fundamental aspects and prospects," *Electrochimica Acta,* vol. 45, p. 2423–2435, 2000.

[53] M. Kusnezoff, "Fuel Cells - Solid Oxide Fuel Cells: Membranes," in *Encyclopedia of Electrochemical Power Sources*, Newnes, Elsevier, 2009, pp. 43-49.

[54] X.-D. Zhou and S. Singhal, "Fuel Cells - Solid Oxide Fuel Cells: Overview," in *Encyclopedia of Electrochemical Power Sources*, Newnes, Elsevier, 2009, pp. 1-16.

[55] A. B. Stambouli and E. Traversa, "Solid oxide fuel cells (SOFCs): a review of an environmentally clean and efficient source of energy," *Renewable and Sustainable Energy Reviews,* vol. 6, pp. 433–455, 2002.

[56] M. Andersson, J. Yuan and B. Sundén, "SOFC modeling considering hydrogen and carbon monoxide as electrochemical reactants," *Journal of Power Sources,* vol. 232, pp. 42-54, 2013.

[57] N. Minh, "Solid oxide fuel cell technology—features and applications," *Solid State Ionics,* vol. 174, p. 271–277, 2004.

[58] Y. Wang, K. Chen, J. Mishler, S. C. Cho and X. C. Adroher, "A review of polymer electrolyte membrane fuel cells: Technology, applications, and needs on fundamental research," *Applied Energy,* vol. 88, pp. 981-1007, 2011.

[59] M. Shojaeefard, G. Molaeimanes, M. Nazemian and M. Moqaddari, "A review on microstructure reconstruction of PEM," *International Journal of Hydrogen Energy,* pp. 1-18, 2016.

[60] C. Wang and J. Appleby, "High-Peak-Power Polymer Electrolyte Membrane Fuel Cells," *Journal of The Electrochemical Society,* vol. 150, no. 4, pp. A493-A498, 2003.

[61] M. Díaz, A. Ortiz and I. Ortiz, "Progress in the use of ionic liquids as electrolyte membranes in fuel cells," *Journal of Membrane Science,* vol. 469, pp. 379–396, 2014.

[62] L. Litster and G. McLean, "PEM fuel cell electrodes," *Journal of Power Sources,* vol. 130, p. 61–76, 2004.

[63] V. Vishnyakov, "Proton exchange membrane fuel cells," *Vacuum,* vol. 80, pp. 1053–1065, 2006.

[64] W. Mohamed and M. H. M. Kamil, "Hydrogen preheating through waste heat recovery of an open-cathode PEM fuel cell leading to power output improvement," *Energy Conversion and Management,* vol. 124, pp. 543–555, 2016.

[65] S. Srinivasan, *Fuel Cells: From Fundamentals to Applications*, New York: Springer Science+Business Media, 2006.

[66] A. Mikolajczuk-Zychora, A. Borodzinski, P. Kedzierzawski, B. Mierzwa, M. Mazurkiewicz-Pawlicka, L. Stobinski, E. Ciecierska, A. Zimoch and M. Opałło, "Highly active carbon supported Pd cathode catalysts fordirect formic acid fuel cells.," *Applied Surface Science,* vol. 388, pp. 645–652, 2016.

[67] M. Shao, "Palladium-based electrocatalysts for hydrogen oxidation," *Palladium-based electrocatalysts for hydrogen oxidation,* vol. 196, pp. 645–652, 2011.

[68] M. Shao, "Electrocatalysis in Fuel Cells," *Catalysts,* vol. 5, pp. 2115-2121, 2015.

[69] A. Valipour, S. Ayyaru and Y. Ahn, "Application of graphene-based nanomaterials as novel cathode catalysts for improving power generation in single chamber microbial fuel cells," *Journal of Power Sources,* vol. 327, pp. 548-556, 2016.

[70] Z. Zhou, "Development of Polymer Electrolyte Membranes for Fuel Cells to Be Operated at High Temperature and Low Humidity," Ph.D. dissertation, Georgia Institute of Technology, 2007.

[71] I. EG&G Technical Services, "Fuel Cell Handbook," U.S. Department of Energy, Morgantown, 2004.

[72] A. Al-Othman, A. Tremblay, W. Pell, S. Letaief, T. Burchell, B. Peppley and M. Ternan, "Zirconium phosphate as the proton conducting material in direct hydrocarbon polymer electrolyte membrane fuel cells operating above the boiling point of water," *Journal of Power Sources,* vol. 195, pp. 2520–2525, 2010.

[73] D. Garraín, Y. Lechón and C. De la Rúa, "Polymer Electrolyte Membrane Fuel Cells (PEMFC) in Automotive Applications: Environmental Relevance of the Manufacturing Stage," *Smart Grid and Renewable Energy,* vol. 2, pp. 68-74, 2011.

[74] A. Dicks, "PEM fuel cells - Applications," in *Comprehensive renewable energy*, Amsterdam, Elsevier, 2012, pp. 203-245.

[75] J. Hirschenhofer, D. Stauffer, R. Engleman and M. Klett, "Fuel Cell Handbook," U.S. Department of Energy, Morgantown, 1998.

[76] R. Kee, H. Zhu and D. Goodwin, "Solid-oxide fuel cells with hydrocarbon fuels," *Proceedings of the Combustion Institute,* vol. 30, pp. 2379–2404, 2005.

[77] V. P. H. Nguyen, A. S. Song, D.-N. Park, H. C. Ham, J. Han, S. P. Yoon, M. R. Othman and J. Kim, "Improved molten carbonate fuel cell performance via reinforced thin anode," *International Journal of Hydrogen Energy,* vol. 37, pp. 16161-16167, 2012.

[78] F. Bidault, D. Brett, P. Middleton, N. Abson and N. Brandon, "An improved cathode for alkaline fuel cells," *International Journal of Hydrogen Energy,* vol. 35, pp. 1783-1788, 2010.

[79] A. Kirubakaran, S. Jain and R. Nema, "A review on fuel cell technologies and power electronic interface," *A review on fuel cell technologies and power electronic interface,* vol. 13, pp. 2430–2440, 2009.

[80] K. Kordesch, V. Hacker, J. Gsellmann, M. Cifrain, G. Faleschini, P. Enzinger, R. Fankhauser, M. Ortner, M. Muhr and R. Aronson, "Alkaline fuel cells applications," *Journal of Power Sources,* vol. 86, pp. 162–165, 2000.

[81] G. McLean, T. Niet, S. Prince-Richard and N. Djilali, "An assessment of alkaline fuel cell technology," *International Journal of Hydrogen Energy,* vol. 27, pp. 507 – 526, 2002.

[82] E. Giilzow, "Alkaline fuel cells: a critical view," *Journal of Power Sources,* vol. 61, pp. 99-104, 1996.

[83] U. E. P. Agency, "Sources of Greenhouse Gas Emissions," Environmental Protection Agency, 2014. [Online]. Available: https://www.epa.gov/ghgemissions/sources-greenhouse-gas-emissions. [Accessed 8 October 2016].

[84] A. Haddad, M. Mannah and H. Bazzi, "Nonlinear time-variant model of the PEM type fuel cell for automotive applications," *Simulation Modelling Practice and Theory,* vol. 51, pp. 31–44, 2015.

[85] A. Alaswad, A. Baroutaji, H. Achour, J. Carton, A. Al Makky and A. Olabi, "Developments in fuel cell technologies in the transport sector," *International Journal of Hydrogen Energy,* vol. 41, pp. 16499-16508, 2016.

[86] T. Wilberforce, A. Alaswad, A. Palumbo, M. Dassisti and A. Olabi, "Advances in stationary and portable fuel cell applications," *International Journal of Hydrogen Energy,* vol. 41, pp. 16509-16522, 2016.

[87] G. Hoogers, *Fuel Cell Technology Handbook*, Danvers, MA: CRC Press, 2003.

[88] B. Cook, "An Introduction to Fuel Cells And Hydrogen Technology," *Engineering Science and Education Journal,* vol. 11, no. 6, pp. 205-216, 2002.

[89] A. Kundu and J. Jang, "Portable Devices: Fuel Cells," in *Encyclopedia of Electrochemical Power Sources*, Amsterdam, Elsevier, 2009, pp. 39-45.

[90] S. Gottesfeld, "Proton Conducting Membrane Fuel Cells II": Proceedings of the Second International Symposium on Proton Conducting Membrane Fuel Cells II, The Electrochemical Society, 1999.

[91] F. M. Hordeski, *Hydrogen and Fuel Cells : Advances in Transportation and Power*, Boca Raton: The Fairmont Press, 2008.

[92] C. Kalamaras and A. Efstathiou, "Hydrogen Production Technologies: Current State and Future Developments," in *Hindawi*, Cyprus, 2013.

[93] Y. Wang, L. Li, L. Hu, L. Zhuang, J. Lu and X. Boqing, "A feasibility analysis for alkaline membrane direct methanol fuel cell: thermodynamic disadvantages versus kinetic advantages," *Electrochemistry Communications,* vol. 5, pp. 662–666, 2003.

[94] P. Cheekatamarla, C. Finnerty and J. Cai, "Internal reforming of hydrocarbon fuels in tubular solid oxide fuel cells," *International Journal of Hydrogen Energy,* vol. 33, pp. 1853 – 1858, 2008.

[95] O. Sharaf and M. Orhan, "An overview of fuel cell technology: Fundamentals and applications," *Renewable and Sustainable Energy Reviews,* vol. 32, pp. 810–853, 2014.

[96] J.-H. Wee, "Which type of fuel cell is more competitive for portable application: Direct methanol fuel cells or direct borohydride fuel cells?," *Journal of Power Sources,* vol. 161, pp. 1-10, 2006.

[97] R. Soltani, M. Rosen and I. Dincer, "Assessment of CO2 capture options from various points in steam methane reforming for hydrogen production," *International Journal of Hydrogen Energy,* vol. 39, no. 35, pp. 20266–20275, 2014.

[98] Y. Zhu, T. Robinson, A. Al-Othman, A. Tremblay and M. Ternan, "n-Hexadecane Fuel for a Phosphoric Acid Direct Hydrocarbon Fuel Cell," *Journal of Fuels,* vol. 2015, pp. 1-9, 2015.

[99] G. Psofogiannakis, Y. Bourgault, B. E. Conway and M. Ternan, "Mathematical model for a direct propane phosphoric acid fuel cell," *Journal of Applied Electrochemistry,* vol. 36, pp. 115–130, 2006.

[100] S. Clarke, A. Dicks, K. Pointon, T. Smith and A. Swann, "Catalytic aspects of the steam reforming of hydrocarbons in internal reforming fuel cells," *Catalysis Today,* vol. 38, pp. 411-423, 1997.

[101] S. Barnett, "Solid Oxide Fuel Cells, Direct Hydrocarbon Type," in *Encyclopedia of Applied Electrochemistry*, New York, Springer Science+Business Media, 2014, pp. 1998-2008.

[102] G. Kaur, Solid Oxide Fuel Cell Components: Interfacial Compatibility of SOFC Glass Seals, Springer International Publishing Switzerland, 2016.

[103] M. Mogensen and K. Kammer, "Conversion Of Hydrocarbons In Solid Oxide Fuel Cells," *Annual Review of Materials Research,* vol. 33, pp. 321–329, 2003.

[104] J. Meusinger, E. Riensche and U. Stimming, "Reforming of natural gas in solid oxide fuel cell systems," *Journal of Power Sources,* vol. 71, pp. 315–320, 1998.

[105] S. McIntosh and R. Gorte, "Direct Hydrocarbon Solid Oxide Fuel Cells," *Chemical Reviews,* vol. 104, no. 10, pp. 4845-4865, 2004.

[106] M. Liu, Y. Choi, L. Yang, K. Blinn, W. Qin, P. Liu and L. Meilin, "Direct octane fuel cells: A promising power for transportation," *Nano Energy ,* vol. 1, no. 3, pp. 448–455, 2012.

[107] S. Park, J. Vohs and R. Gorte, "Direct oxidation of hydrocarbons in a solid-oxide fuel cell," *Nature,* vol. 404, pp. 265-267, 2000.

[108] A. Al-Othman, A. Tremblay, W. Pell, S. Letaief, Y. Liu, B. Peppley and M. Ternan, "A modified silicic acid (Si) and sulphuric acid (S)eZrP/PTFE/glycerol composite membrane for high temperature direct hydrocarbon fuel cells," *Journal of Power Sources,* vol. 224, pp. 158-167, 2013.

[109] O. Savadogo and F. J. Rodriguez Varela, "Low-temperature direct propane polymer electrolyte membranes fuel cell (DPFC)," *Journal of New Materials for Electrochemical Systems,* vol. 4, pp. 93-97, 2001.

[110] H. Khakdaman, Y. Bourgault and M. Ternan, "Computational modeling of a direct propane fuel cell," *Journal of Power Sources,* vol. 196, pp. 3186–3194, 2011.

[111] M. Perry, F. McLarnon, J. Newman and E. Cairns, "Exploratory Fuel-Cell Research: I. Direct-Hydrocarbon Polymer-Electrolyte Fuel Cell, II. Mathematical Modeling of Fuel-Cell Cathodes," Energy and Environment Division, 1996.

[112] F. Rodríguez Varela and O. Savadogo , "The Effect of Anode Catalysts on the Behavior of Low Temperature Direct Propane Polymer Electrolyte Fuel Cells (DPFC)," *Journal of New Materials for Electrochemical Systems,* vol. 9, pp. 127-137 , 2006.

[113] C. Yang., P. Costamagna, S. Srinivasan, J. Benziger and A. Bocarsly, "Approaches and technical challenges to high temperature operation of proton exchange membrane fuel cells," *Journal of Power Sources,* vol. 103, no. 1, pp. 1-9, 2001.

[114] X. Gang, L. Qingfeng, H. A. Hjuler and N. Bjerrum, "Hydrogen Oxidation on Gas Diffusion Electrodes for Phosphoric Acid Fuel Cells in the Presence of Carbon Monoxide and Oxygen," *Journal of The Electrochemical Society,* vol. 142, no. 9, pp. 2890-2893, 1995.

[115] C. Yang, S. Srinivasan, A. Bocarsly, S. Tulyani and J. Benziger, "A comparison of physical properties and fuel cell performance of Nafion and zirconium

phosphate/Nafion composite membranes," *Journal of Membrane Science,* vol. 237, no. 1-2, pp. 145-161, 2004.

[116] FuelCellStore, "Considerations for Fuel Cell Design," 5 November 2017. [Online]. Available: http://www.fuelcellstore.com/blog-section/considerations-for-fuel-cell-design.

[117] D. Ramdutt, C. Charles, J. Hudspeth, B. Ladewig, T. Gengenbach, R. Boswell, A. Dicks and P. Brault, "Low energy plasma treatment of Nafion® membranes for PEM fuel cells," *Journal of Power Source,* vol. 165, pp. 41–48, 2007.

[118] P. Choi, "Investigation of Thermodynamic and Transport Properties of Proton-Exchange Membranes in Fuel Cell Applications," Ph.D. dissertation, Worcester Polytechnic Institute, 2004.

[119] A. Alberti, M. Casciola, U. Costantino, G. Levi and G. Ricciardi, "On the Mechanism of Diffusion and Ionic Transport in Crystalline Insolubke Acid Salts of Tetravalent Metals I," *Journal of Inorganic and Nuclear Chemistry,* vol. 40, pp. 533-537, 1978.

[120] C. Amphlett, L. McDonald, and M. Redman, "Synthetic inorganic ion-exchange materials—I zirconium phosphate," *Journal of Inorganic and Nuclear Chemistry,* vol. 6, no. 3, p. 220–235, 1958.

[121] R. Hamlen, "Ionic Conductivity of Zirconium Phosphate," *Journal of the Electrochemical Society,* vol. 109, no. 8, pp. 746-749, 1962.

[122] G. Alberti, M. Casciola, U. Costantino, G. Levi and G. Ricciardi, "Electrical Conductance of Zirconium Bis (Monohydrogen Ortho-Phosphate) Monohydrate With a Layered Structure," *Journal of Inorganic and Nuclear Chemistry,* vol. 40, pp. 533-537, 1978.

[123] W. G. Grot and G. Rajendran, "Membranes containing inorganic fillers and membrane and electrode assemblies and electrochemical cells employing same". United States of America Patent US5919583 A, 6 July 1999.

[124] G. Alberti and M. Casciola, "Solid state protonic conductors, present main applications and future prospects," *Solid State Ionics,* vol. 145, pp. 3-16, 2001.

[125] W. Hogarth, D. Da Costa and G. M. Lu, "Solid acid membranes for high temperature (140° C) proton exchange membrane fuel cells," *Journal of Power Sources,* vol. 142, no. 1-2, pp. 223-237, 2005.

[126] P. Jerus and A. Clearfield, "Ionic conductivity of anhydrous zirconium bis(monohydrogen orthophosphate) and its sodium ion forms," *Solid State Ionics,* vol. 6, no. 1, pp. 79-83, 1982.

[127] G. Alberti and M. Casciola , "Layer Hydrates," in *Proton conductors : solids, membranes, and gels--materials and devices*, New York, Cambridge University Press, 1992, pp. 238-251.

[128] G. Alberti and M. Casciola, "Layered metalIV phosphonates, a large class of inorgano-organic proton conductors," *Solid State Ionics,* vol. 97, no. 1-4, pp. 177-186, 1997.

[129] H. Ye, J. Huang, J. Xu, N. Kodiweera, J. Jayakody and S. Greenbaum, "New membranes based on ionic liquids for PEM fuel cells at elevated temperatures," *Journal of Power Sources,* vol. 178, pp. 651–660, 2008.

[130] A. Diedrichs and J. Gmehling, "Measurement of heat capacities of ionic liquids by differential scanning calorimetry," *Fluid Phase Equilibria,* vol. 244, pp. 68–77, 2006.

[131] M. Yoshizawa-Fujita, K. Johansson, P. Newman, D. MacFarlane and M. Forsyth, "Novel Lewis-base ionic liquids replacing typical anions," *Tetrahedron Letters,* vol. 47, pp. 2755–2758, 2006.

[132] m. armand, F. endres, d. macFarlane, h. ohno and B. scrosati, "ionic-liquid materials for the electrochemical challenges of the future," *Nature Materials,* vol. 8, pp. 621-629, 2009.

[133] D. MACFARLANE, M. FORSYTH, P. HOWLETT, J. PRINGLE, J. SUN, G. ANNAT, W. NEIL and E. IZGORODINA, "Ionic Liquids in Electrochemical Devices and Processes: Managing Interfacial Electrochemistry," *Accounts of Chemical Research,* vol. 40, pp. 1165–1173, 2007.

[134] K. Hooshyari, M. Javanbakht and M. Adibi, "Novel composite membranes based on PBI and dicationic ionic liquids for high temperature polymer electrolyte membrane fuel cells," *Electrochimica Acta,* vol. 205, pp. 142–152, 2016.

[135] M. Díaz, A. Ortiz and I. Ortiz, "Progress in the use of ionic liquids as electrolyte membranes in fuel cells," *Journal of Membrane Science,* vol. 469, pp. 379–396, 2014.

[136] M. Doyle, S. Choi and G. Proulx, "High-Temperature Proton Conducting Membranes Based on Perfluorinated Ionomer Membrane-Ionic Liquid Composites," *Journal of The Electrochemical Society,* vol. 147, no. 1, pp. 34-37, 2000.

[137] W. Li, F. Zhang, S. Yi, C. Huang, H. Zhang and M. Pan, " Effects of casting solvent on microstructrue and ionic conductivity of anhydrous sulfonated poly(ether ether ketone)-inoic liquid composite membranes," *International Journal of Hydrogen Energy,* vol. 37, pp. 748-754, 2012.

[138] S. Smeets, L. Liu, J. Dong and L. McCusker, "Ionothermal Synthesis and Structure of a New Layered Zirconium Phosphate," *Inorganic Chemistry,* vol. 54, no. 16, pp. 7953–7958, 2015.

[139] D. Gui, T. Zheng, J. Xie, Y. Cai, Y. Wang, L. Chen, J. Diwu, Z. Chai and S. Wang, "Significantly Dense Two-Dimensional Hydrogen-Bond Network in a Layered Zirconium Phosphate Leading to High Proton Conductivities in Both Water-Assisted Low-Temperature and Anhydrous Intermediate-Temperature Regions," *Inorganic Chemistry,* vol. 55, pp. 12508−12511, 2016.

[140] A. Al-Othman, A. Tremblay, W. Pell, Y. Liu, B. Peppley and M. Ternan, "The effect of glycerol on the conductivity of Nafion-free ZrP/PTFE composite membrane electrolytes for direct hydrocarbon fuel cells," *Journal of Power Sources,* vol. 199, pp. 14-21, 2012.

[141] A. Pereiro , J. Araújo, F. Oliveira, C. Bernardes, J. Esperança, J. Lopes, I. Marrucho and L. Rebelo, "Inorganic salts in purely ionic liquid media: the development of High Ionicity Ionic Liquids (HIILs)," *Chemical Communications,* vol. 48, no. 30, pp. 3656-3658, 2012.

[142] H. Almeida, J. Canongia Lopes, L. Rebelo, J. P. Coutinho, M. Freire and I. Marrucho, "Densities and Viscosities of Mixtures of Two Ionic Liquids Containing a Common Cation," *Journal of Chemical & Engineering Data,* vol. 61, no. 8, pp. 2828–2843, 2016.

[143] O. Zech, A. Stoppa, R. Buchner and W. Kunz, "The Conductivity of Imidazolium-Based Ionic Liquids from (248 to 468) K. B. Variation of the Anion," *Journal of Chemical & Engineering Data,* vol. 55, no. 5, pp. 1774–1778, 2010.

[144] A. Nazet, S. Sokolov, T. Sonnleitner, T. Makino, M. Kanakubo and R. Buchner, "Densities, Viscosities, and Conductivities of the Imidazolium Ionic Liquids [Emim][Ac], [Emim][FAP], [Bmim][BETI], [Bmim][FSI], [Hmim][TFSI], and [Omim][TFSI]," *Journal of Chemical & Engineering Data,* vol. 60, no. 8, pp. 2400–2411, 2015.

[145] H. Rodríguez and J. Brennecke, "Temperature and Composition Dependence of the Density and Viscosity of Binary Mixtures of Water + Ionic Liquid," *Journal of Chemical & Engineering Data,* vol. 51, no. 6, p. 2145–2155, 2006.

[146] iolitec, "Technical Data Sheet:Diethylmethylammonium methanesulfonate," iolitec, 2014. [Online]. Available: https://iolitec.de/sites/iolitec.de/files/sds.

[147] T. Yasuda, H. Kinoshita, M. Shah Miran and M. Watanabe, "Comparative Study on Physicochemical Properties of Protic Ionic Liquids Based on Allylammonium and Propylammonium Cations," *Journal of Chemical & Engineering Data,* vol. 58, no. 10, pp. 2724-2732, 2013.

[148] "Sigma-Aldrich," [Online]. Available: http://www.sigmaaldrich.com/catalog/product. [Accessed 31 October 2017].

[149] I. L. D. -. ILThermo, "NIST Standard Reference Database #147," [Online]. Available: http://ilthermo.boulder.nist.gov/. [Accessed 31 October 2017].

[150] G. Alberti, M. Casciola, U. Costantino, G. Levi and G. Ricciardi, "On the Mechanism of Diffusion and Ionic Transport in Crystalline Insoluble Acid Salts of Tetravalent Metals," *Journal of Inorganic and Nuclear Chemistry,* vol. 40, pp. 533-537, 1978.

[151] B. Casañas-Montes, A. Díaz, C. Barbosa, C. Ramos, C. Collazo, E. Meléndez, C. Queffelec, F. Fayon, A. Clearfield, B. Bruno and J. Colóna, "Molybdocene dichloride intercalation into zirconium phosphate nanoparticles," *Journal of Organometallic Chemistry,* vol. 791, pp. 34-40, 2015.

[152] K. Hooshyari, M. Javanbakht and M. Adibi, "Novel composite membranes based on PBI and dicationic ionic liquids for high temperature polymer electrolyte membrane fuel cells," *Electrochimica Acta,* vol. 205, pp. 2016, 142–152.

[153] P. Hunt, C. Ashworth and R. Matthews, "Hydrogen bonding in ionic liquids," *Chemical Society Reviews,* vol. 44, no. 5, pp. 1257-1288, 2015.

[154] M. Rani, A. Brandt, L. Crowhurst, A. Dolan, N. Hassan, J. Hallett, P. Hunt, M. Lui, H. Niedermeyer, J. Perez-Arlandis, M. Schrems, T. To, T. Welton and R. Wilding, "Understanding the Polarity of Ionic Liquids," *Physical Chemistry Chemical Physics,* vol. 13, no. 37, pp. 16831-16840 , 2011.

[155] U. Baig, W. Wani and L. Ting Hun, "Facile synthesis of electrically conductive polycarbazole-zirconium(IV)phosphate cation exchange nanocomposite and its room temperature ammonia sensing performance," *New Journal of Chemistry,* vol. 39, no. 9, pp. 6882-6891, 2015.

[156] D. Bykov, R. Konings, C. Apostolidis, A. Hen, E. Colineau, T. Wiss and P. Raison, "Synthesis and investigation of neptunium zirconium phosphate, a member of the NZP family: crystal structure, thermal behaviour and Mössbauer spectroscopy studies," *Royal Society of Chemistry,* vol. 46, no. 35, pp. 11626-11635, 2017.

[157] I. Amaral, P. Granja and M. Barbosa, "Chemical modification of chitosan by phosphorylation: an XPS, FT-IR and SEM study," *Journal of Biomaterials Science, Polymer Edition ,* vol. 16, no. 12, pp. 1575–1593, 2005.

[158] S. Horsley, D. Nowell and D. Stewart, "The infrared and Raman spectra of α-zirconium phosphate," *Spectrochimica Acta Part A: Molecular Spectroscopy,* vol. 30, no. 2, pp. 535-541, 1974.

[159] J. T.-W. Wang and S. L.-C. Hsu, "Enhanced high-temperature polymer electrolyte membrane for fuel cells based on polybenzimidazole and ionic liquids," *Electrochimica Acta,* vol. 56, pp. 2842–2846, 2011.

[160] M. Garcia, J. Naffin, N. Deng and T. Mallouk, "Preparative-Scale Separation of Enantiomers Using Intercalated a-Zirconium Phosphate," *Chemistry of Materials,* vol. 7, pp. 1968 - 1973, 1995.

[161] P. Colomban, "Nature of the Protonic Species and the Gel-crystal Transition in Hydrated Zirconium Phosphate," *Journal of Molecular Structure,* vol. 198, pp. 271-295, 1989.

[162] U. o. N. Florida, "Chapter 2 - Physical Methods for Characterizing Solids," [Online]. Available: https://www.unf.edu/~michael.lufaso/chem4627/ch2_solid_state.pdf. [Accessed 31 October 2017].

[163] A. Clearfield and J. Stynes, "The preparation of crystalline zirconium phosphate and some observations on its ion exchange behaviour," *Journal of Inorganic and Nuclear Chemistry,* vol. 26, no. 1, pp. 117-129, 1964.

[164] M. Casciola, A. Donnadio, F. Montanari, P. Piaggio and V. Valentini, "Vibrational spectra and H-bondings in anhydrous and monohydrate a-Zr phosphates," *Journal of Solid State Chemistry,* vol. 180, pp. 1198–1208, 2007.

[165] P. L. Stanghellini, E. Boccaleri, E. Diana, G. Alberti and R. Vivani, "Vibrational Study of Some Layered Structures Based on Titanium and Zirconium Phosphates," *Inorganic Chemistry,* vol. 43, pp. 5698−5703, 2004.

[166] A. Anantaraman and C. Gardner, "Studies on ion-exchange membranes. Part 1. Effect of humidity on the conductivity of Nafion," *Journal of Electroanalytical Chemistry,* vol. 414, pp. 115-120, 1996.

[167] Y. Ye, X. Wu, Z. Yao, L. Wu, Z. Cai, L. Wang, X. Ma, Q.-H. Chen, Z. Zhang and S. Xiang, "Metal-Organic Frameworks with Large Breathing Effect to Host Hydroxyl Compounds for High Anhydrous Proton Conductivity over a Wide Temperature Range from Subzero to 125 oC," *Journal of Materials Chemistry A,* vol. 4, pp. 4062-4070 , 2016.

[168] M. Pagliaro and M. Rossi, "The Future of Glycerol: New Uses of a Versatile Raw Material," in *RSC Green Chemistry*, Springer, 2008, pp. 1-17.

Vita

Hanin Mohammed was born in September 27th, 1993, in Jordan. She received her primary education in Amman, Jordan and her secondary education in Sharjah, UAE. She Joined the American University of Sharjah in 2011 to pursue a Bachelor of science in Chemical Engineering. She received her bachelor degree of Chemical Engineering with a cum laude honor in June 2015. In September 2015, she joined the Chemical Engineering master's program in the American University of Sharjah in which she worked as a graduate teaching assistant.